Digital Comprehensive Summaries of Uppsala Dissertations
from the Faculty of Science and Technology 2611

Revealing Glacier Bed Topography from Regional to Global Scales

THOMAS FRANK

ACTA UNIVERSITATIS
UPSALIENSIS
2026

ISSN 1651-6214
ISBN 978-91-513-2665-8
urn:nbn:se:uu:diva-570124

UPPSALA
UNIVERSITET

Dissertation presented at Uppsala University to be publicly examined in Hambergsalen, Geocentrum, Villavägen 16, Uppsala, Friday, 6 February 2026 at 10:00 for the degree of Doctor of Philosophy. The examination will be conducted in English. Faculty examiner: Professor Guðfinna Aðalgeirsdóttir (University of Iceland, School of Engineering and Natural Sciences, Faculty of Earth Sciences, Reykjavik, Iceland).

Abstract

Frank, T. 2026. Revealing Glacier Bed Topography from Regional to Global Scales. *Digital Comprehensive Summaries of Uppsala Dissertations from the Faculty of Science and Technology* 2611. 81 pp. Uppsala: Acta Universitatis Upsaliensis. ISBN 978-91-513-2665-8.

Mountain glaciers and ice caps distinct from the ice sheets in Greenland and Antarctica, hereafter "glaciers", are melting and retreating around the World. Improving projections of glacier change and assessing associated Earth system impacts requires accurate knowledge of the bed topography beneath the ice. However, direct observations of the glacier bed exist for only a small fraction of the >200,000 glaciers globally. Thus, computational inversion methods are needed to infer bed properties from more accessible surface data. This thesis presents the development of a glacier bed and ice thickness inversion method and its applications on regional and global scales.

The newly developed inverse method is computationally efficient, robust, model agnostic and compatible with complex ice-flow physics on distributed grids. Tests on synthetic and real glaciers demonstrated strong performance, with benchmarks ranking it among the best available methods. The first regional application produced detailed bed topographies for Scandinavia, constraining total glacier volume to 0.32×10^3 km^3, equivalent to 0.8 mm of global mean sea-level rise if melted. A subsequent application to all glaciers in Svalbard — where glacier dynamics are more complex — estimated a volume of 6.80×10^3 km^3 (16.3 mm sea-level equivalent) and achieved improved agreement with observations compared to earlier studies. Finally, a global application yielded a total glacier volume of 149.41×10^3 km^3 (316.1 mm sea-level equivalent). While the global total aligns with previous estimates, notable regional differences were identified. Beyond ice volume, the global study produced physically realistic bed topographies and mapped >50,000 potential future lakes in presently glacier-covered terrain, totaling 3,138 km^3 in volume (2% of global glacier volume) and >40,000 km^2 in area.

Methodologically, this thesis advances large-scale glacier thickness inversions, and presents the first global-scale application of higher-order ice-flow physics on distributed grids, enabled by physics-informed deep learning and parallelized code optimized for Graphic Processing Units. Practically, the regional and global ice volume estimates provide key data for adaptation and mitigation strategies in response to glacier mass loss and sea-level rise, while the derived bed maps support future research across the Earth sciences and improved projections of glacier change.

Keywords: Glacier, Climate Change, Inversion, Machine Learning, Sea level rise, Topography, Modeling, Lakes, Svalbard, Field work.

Thomas Frank, Department of Earth Sciences, LUVAL, Villav. 16, Uppsala University, SE-75236 Uppsala, Sweden.

ISSN 1651-6214
ISBN 978-91-513-2665-8
URN urn:nbn:se:uu:diva-570124 (http://urn.kb.se/resolve?urn=urn:nbn:se:uu:diva-570124)

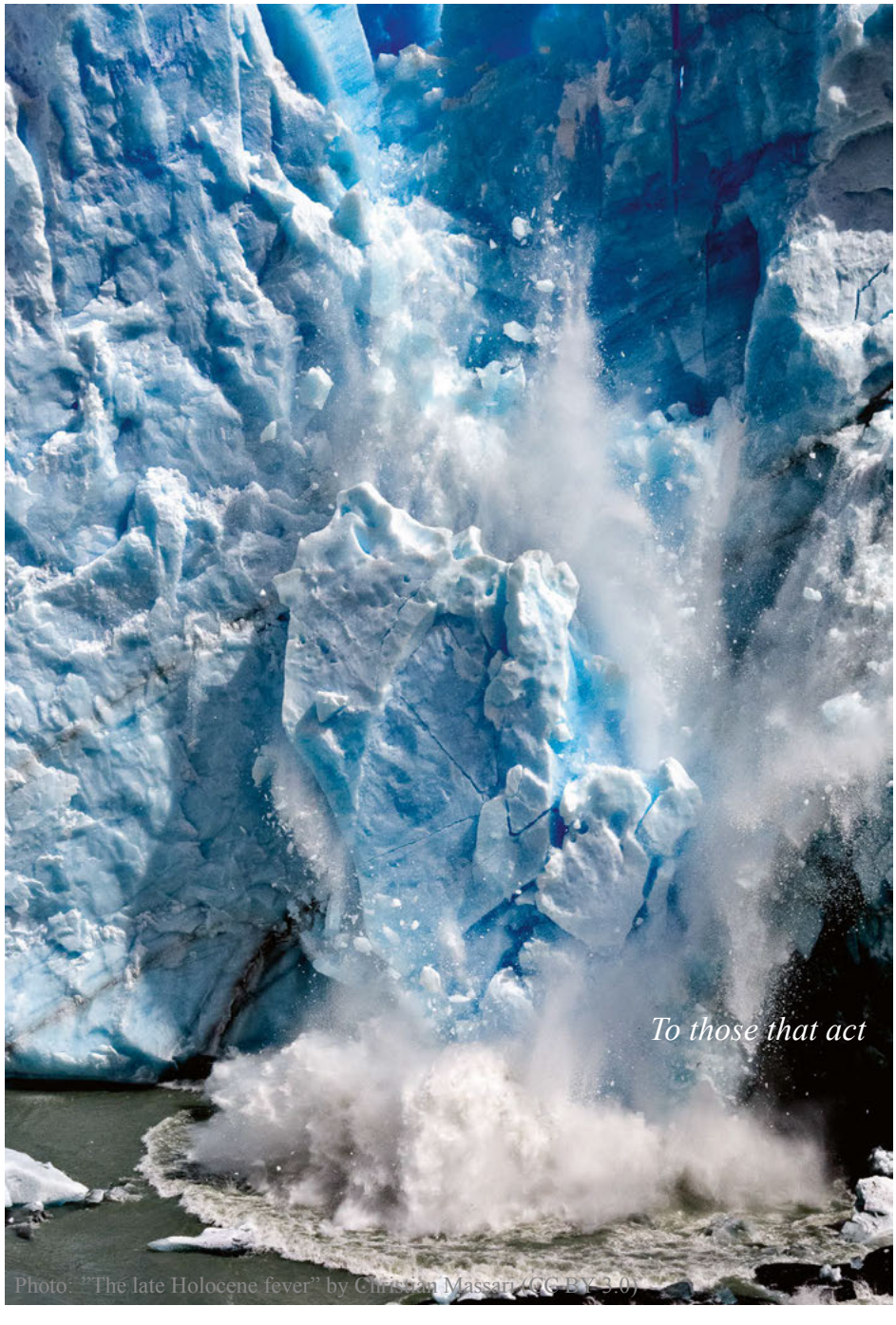

List of papers

This thesis is based on the following papers, which are referred to in the text by their Roman numerals.

I **Frank, T.**, Van Pelt, W. J. J., and Kohler, J.: Reconciling ice dynamics and bed topography with a versatile and fast ice thickness inversion, The Cryosphere, 17, 4021–4045, https://doi.org/10.5194/tc-17-4021-2023, 2023.

II **Frank, T.** and Van Pelt, W. J. J.: Ice volume and thickness of all Scandinavian glaciers and ice caps, Journal of Glaciology, 1–14, https://doi.org/10.1017/jog.2024.25, 2024.

III Van Pelt, W.* and **Frank, T.***: New glacier thickness and bed topography maps for Svalbard, The Cryosphere, 19, 1–17, https://doi.org/10.5194/tc-19-1-2025, 2025.
*both authors contributed equally to this work

IV **Frank, T.**, Van Pelt, W. J. J., Rounce, D. R., Jouvet, G., and Hock, R.: Unveiling the hidden lake-rich landscapes under Earth´s Glaciers, *in review*, 2025.

Author Contributions

My contributions[1] to Papers I-IV:

In Papers I, II, and IV the author had the main responsibility for conceptualisation, data curation, formal analysis, investigation, methodology, software, validation, visualisation, and writing of the original manuscripts, as well as review and editing. In Paper III with two main authors, these tasks were shared equally with the other main author.

During my doctoral studies, I also contributed to the following papers, which are not included in this thesis:

> **Frank, T.**, Åkesson, H., de Fleurian, B., Morlighem, M., and Nisancioglu, K. H.: Geometric controls of tidewater glacier dynamics, The Cryosphere, 16, 581–601, https://doi.org/10.5194/tc-16-581-2022, 2022.
>
> Helama, S., Herva, H., Arppe, L., Gunnarson, B., **Frank, T.**, Holopainen, J., Nöjd, P., Mäkinen, H., Mielikäinen, K., Sutinen, R., Timonen, M., Uusitalo, J., and Oinonen, M.: Disentangling the Evidence of Milankovitch Forcing From Tree-Ring and Sedimentary Records, Front. Earth Sci., 10, https://doi.org/10.3389/feart.2022.871641, 2022.
>
> Helama, S., Saarinen, T., Suominen, T., Fuentes, M., **Frank, T.**, and Gunnarson, B.: An integration of μXRF and X-ray microdensitometry records in dendrochronology, Dendrochronologia, 86, 126229, https://doi.org/10.1016/j.dendro.2024.126229, 2024.
>
> Wang, Z., Ross, N., **Frank, T.**, Barnett, J., Santin, I., Houssais, M., Dahlkvist, J., and Kirchner, N.: Ice thickness and subglacial topography of Swedish reference glaciers revealed by radio-echo sounding, *submitted*, 2025.

[1] According to the contributor Roles Taxonomy (CRediT), `https://credit.niso.org/`

Contents


Salajekna
Sweden
Photo: Thomas Frank

1. Introduction

Glaciers and ice sheets are critical components of the Earth system. They play a central role in regulating global sea levels, storing freshwater, and shaping landscapes. Indeed, the waxing and waning of glaciers and ice sheets has left a profound imprint on Earth's history, with ice in Antarctica and Greenland having persisted continuously for at least $\sim$34 and $\sim$1 million years, respectively (Zachos et al., 2001; Schaefer et al., 2016; Christ et al., 2021). In the face of global anthropogenic climate warming, glaciers and ice sheets are now entering an era of mass loss and retreat that may lead to large-scale disappearance of glaciers and the disintegration of entire ice sheets (IPCC, 2021).

This thesis focuses on ice caps and mountain glaciers distinct from the ice sheets in Greenland and Antarctica, hereafter referred to as "glaciers" only (Fig. 1.1). Although small in area and volume compared to the Greenland and Antarctic ice sheets, these glaciers currently contribute about half of the total land ice input to global sea-level rise (Hugonnet et al., 2021). Glacier melt has, in recent decades, exceeded the contributions from either of the much larger ice sheets (Zemp et al., 2025), making it a dominant and highly dynamic driver of sea-level change in the near term.

The comparatively fast glacier response is due to differences in size and mass turnover rates. Whereas ice sheets are vast ice masses, by definition larger than 50,000 km^2 (Cogley et al., 2010), and often feature dry inland areas, glaciers are typically much smaller and exhibit larger mass balance gradients — that is, stronger contrasts in the net gain or loss of ice between high-elevation accumulation areas and low-elevation ablation areas — resulting in correspondingly shorter mass turnover times. Despite covering only 0.5% of the global land area (Fig. 1.1a; RGI Consortium, 2017), glaciers modulate a range of Earth system processes from a local to a global scale: they create a small-scale microclimate (Oerlemans, 2010), they host cold-adapted species (Skidmore et al., 2000; Hodson et al., 2008), they produce and redistribute sediment (Elverhøi et al., 1983; Hodson and Ferguson, 1999), they reshape landscapes (Stroeven et al., 2016; Cordonnier et al., 2023), including the creation of overdeepenings which can host lakes upon glacier retreat (Linsbauer et al., 2016; Zheng et al., 2021; Zhang et al., 2022), their meltwater contributes to streamflow in river systems and acts as a buffer during droughts (Xu et al., 2009; Huss and Hock, 2018; Immerzeel et al., 2020), and ultimately they hold back water otherwise contributing to global sea level (Farinotti et al., 2019a; Millan et al., 2022). As glaciers retreat, affected systems are now undergoing rapid changes: sea levels are rising (Edwards et al., 2021), buffering capacities

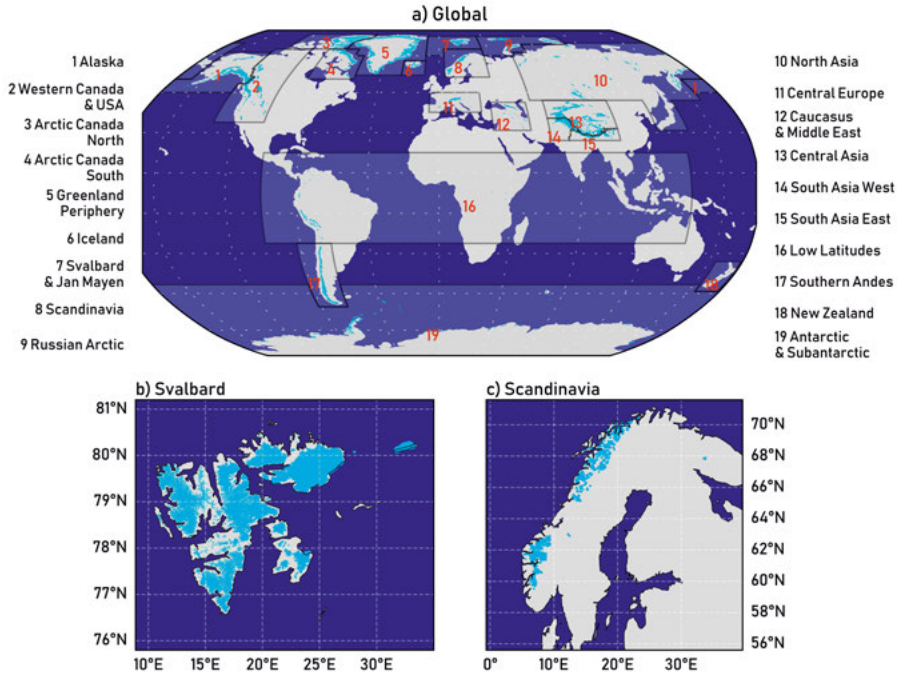

Figure 1.1. Overview of global glacier cover. a) Location of all glaciers on Earth (light blue) with 19 numbered glacier regions defined by RGI Consortium (2017) indicated by boxes and red numbers. The name of the glacier regions are given next to the figure. b) Glacier cover in Svalbard. c) Glacier cover in Scandinavia. Note that in c), for reasons of readability, the size of the light blue markers is exaggerated and does not reflect the actual size of the glaciers. This is different from b) where the light blue area represents the actual glacier cover in Svalbard to scale.

are being depleted (Immerzeel et al., 2020), mountain hazards, such as glacier lake outburst floods or landslides, are increasing (Liu et al., 2021; Sattar et al., 2025), and topographic changes are occurring on a landscape scale (Kavan et al., 2023).

1.1 Global and regional glacier changes in a warming climate

The Arctic archipelago of Svalbard (Fig. 1.1b), one study region of this thesis, exemplifies this rapid change. It is among the fastest-warming regions on the planet, experiencing pronounced Arctic amplification due to sea-ice loss and associated feedbacks (Serreze and Barry, 2011; Bintanja and van der Linden, 2013). Between 1961/62 and 2015/16, glaciers in Svalbard and Jan Mayen alone contributed about 7% of the total glacier-driven sea-level rise (IPCC,

2021). Meanwhile, glaciers in regions showing near-balanced mass budgets until recently have also shifted to a mass loss regime, such as in Scandinavia, another study region in this thesis (Fig. 1.1c; here defined as in RGI Consortium (2017), i.e. comprising all glaciers in Fennoscandia). After a period of both mass losses and gains from the 1960s to the 1990s (Andreassen et al., 2020), observations since 2000 indicate a cumulative loss of 40 Gt until 2023, equivalent to roughly one eighth of their mass (Zemp et al., 2025). Aggregated on a global scale, glaciers have lost mass at a rate of 273 Gt yr^{-1} over the period 2000 - 2023 (cumulative total: 6,542 Gt), with a 36% increase in loss observed in the latter half of the period (Zemp et al., 2025). This places their sea-level contribution at 20% of the observed global mean sea-level rise (absolute value: 18.05 mm), second only to ocean water expansion.

Projections of future glacier change suggest an acceleration of mass loss in the near-term which will only decelerate once glaciers have stabilized at higher elevations or disappeared completely (Rounce et al., 2023; Zekollari et al., 2025). The primary control on future glacier evolution is the trajectory of anthropogenic greenhouse gas emissions: Under a Paris agreement-aligned scenario with 1.5°C global warming relative to pre-industrial, glaciers globally will lose 26% of their mass until 2100 (Rounce et al., 2023), and 47% by the time they have fully equilibrated with the new climate (Zekollari et al., 2025). In contrast, under warming of 4°C, 41 and 86% of glacier mass will be lost in this century and in the long-term, respectively. A substantial proportion of mass loss is effectively unavoidable (so-called committed mass loss): should climate warming stabilize at present-day levels, 39% of global glacier mass would still be lost long-term (Zekollari et al., 2025). Importantly, temperature overshoot scenarios where temperatures rise above and later return below 1.5°C warming lead to significantly larger mass loss over a multi-centennial timescale compared to consistently limiting warming at this level, due to the non-linear response of glaciers to temperature perturbations and hysteresis effects, such as the mass balance - elevation feedback (Schuster et al., 2025). In Svalbard and Scandinavia, glaciers are particularly vulnerable to present and future warming due to their hypsometric distribution with low elevation ranges (Noël et al., 2020; Zekollari et al., 2025): 46 and 66% mass loss are already committed in these two regions, respectively (Zekollari et al., 2025). Under both intermediate and high emission scenarios, model projections suggest that Svalbard's glaciers will lose more than 50 Gt yr^{-1} by 2060 through surface processes alone (van Pelt et al., 2021) - a scenario already preempted by the record 2024 melt season with a total loss of $\sim$62 Gt (Schuler et al., 2025). In Scandinavia, warming beyond 2°C will result in largely ice-free conditions already by the end of this century (Rounce et al., 2023; Zekollari et al., 2025).

1.2 Relevance of subglacial topography

In light of these trends, scientific efforts have increasingly focused on refining projections of future glacier evolution and quantifying the associated environmental and societal impacts. Despite major advances, the above projections rely on boundary conditions that, in parts, are still poorly constrained, introducing substantial uncertainty into estimates of glacier change. A particularly critical gap concerns the insufficiently known shape of glaciers beds and the associated uncertain spatial distribution of glacier ice, from individual glaciers to global scales (Hock et al., 2023). Prognostic glacier and ice-sheet models depend on realistic bed geometries for model initialization, yet errors in these inputs remain a major source of uncertainty, in particular in short- and medium-term projections (Cook et al., 2023b; Zekollari et al., 2025). Similarly, the poor agreement among existing global and regional ice volume estimates hinders the accurate quantification of glaciers' potential contribution to future sea-level rise (IPCC, 2021). Beyond the climate system, inaccurate bed topographies limit assessments of future freshwater availability from glacial reservoirs in regions such as High Mountain Asia and the Andes (Pritchard, 2019; Immerzeel et al., 2020), and impede evaluations of the post-glacial landscapes that will emerge, with implications for hydropower planning (Farinotti et al., 2019b; Ekblom Johansson et al., 2022), ecosystem succession (Bosson et al., 2023), and natural hazard risk (Abdel-Fattah et al., 2024). This thesis seeks to address these gaps by reconstructing regional and global ice thickness and subglacial topography, along with corresponding estimates of glacier volume and sea-level equivalent (SLE). By fulfilling these aims, this work provides the physical basis for more accurate projections of glacier mass loss and sea-level rise, enables improved initialization of prognostic glacier models, and supports planning for freshwater resources and landscape adaptation in a warming world.

The key conundrum at the base of this work is the inaccessibility of the glacier bed. Despite advances in geophysical techniques commonly used to observe it, i.e. predominantly ground-penetrating radar (GPR; Bogorodsky et al., 1985), through, for instance, the increasing ability to conduct air-borne surveys (Grab et al., 2021), observations cannot be obtained in sufficient spatial coverage so as to make them useful by themselves towards the above overarching research questions. Indeed, only roughly 2% of all glaciers worldwide have any thickness observations (Welty et al., 2020), and even on those, large gaps between survey lines are the norm. This is not expected to change substantially in the foreseeable future due to the logistical challenges and costs associated with GPR field campaigns (Bogorodsky et al., 1985). Notably, there is to-date no possibility of obtaining ice thickness measurements from space using radar because the low-frequency electromagnetic waves required are reflected or strongly distorted by Earth's ionosphere (Freeman et al., 2017). Therefore, computational inversion techniques are needed that use available surface ob-

servations alongside models of the ice flow process to reconstruct the properties of the glacier bed (MacAyeal, 1993). The recent years have seen the development of multiple such methods (Farinotti et al., 2017, 2021), two of which have been applied on a global scale (Farinotti et al., 2019a; Millan et al., 2022). Although agreeing on the total global ice volume, they show large differences on regional scales, highlighting the uncertainty in these products. In addition, the bed topography maps they obtained are known to be partly unrealistic and at odds with our physical understanding of ice flow (Huss and Farinotti, 2012), hampering their wider applicability, such as for catchment studies in hydrology. This is directly linked to several simplifications in the methodology of these works, grounded in computational limitations that formed prohibitive constraints until recently (Farinotti et al., 2019a; Millan et al., 2022). This thesis presents a novel computational inversion technique that was used in conjunction with recently developed machine-learning techniques to model the ice thickness and bed topography on regional and global scales with high physical fidelity, overcoming several challenges faced by previous studies. The different chapters of this thesis collectively represent the progression of the inversion technique — from method formulation and validation on several artificial and one real glacier, to application in a region of land-terminating glaciers, followed by a larger and more complex region containing marine-terminating and surging glaciers, and finally to a global-scale implementation encompassing all glaciers on Earth.

Returning from
Stour Räitaglaciären
Sweden

Photo: Thomas Frank

2. Research Aims

There is a pressing need to constrain the ice thickness, volume and basal topography of glaciers - both to improve glacier mass loss projections, and to assess the consequences of glacier retreat. Addressing this challenge at large spatial scales and with high physical fidelity, thus improving existing bed topography products, constitutes the central focus of this thesis. Accordingly, the research aims of this work are to:

1. Develop an ice thickness inversion method that is computationally fast, compatible with complex ice-flow physics, and capable of producing spatially distributed thickness maps.
2. Establish a framework for applying the method at regional scales and demonstrate its applicability to all types of glaciers observed on Earth.
3. Generate a global dataset of subglacial topography and ice thickness, and derive updated estimates of total glacier volume and associated SLE.

Lomonosovfonna
Svalbard

Photo: Thomas Frank

3. Background

This chapter provides theory and background information on key concepts that form the backbone of this thesis. These include ice flow modeling, using both classical physical approaches and newer machine-learning based methods, inversion techniques applied in the field of glaciology and the concept of large-scale glacier modeling.

3.1 Ice flow modeling

Given the lack of bed observations for most glaciers worldwide, computational inversion methods are needed which rely on process modeling of how comparatively easily obtainable surface observations relate to the unknown properties of the glacier bed. The governing process in this context is ice flow - the slow viscous deformation of ice under the force of gravity modulated by the shape of the glacier bed which determines the observed surface geometry and flow velocity. Our knowledge of this process is expressed through equations that derive from the fundamental physical concepts of mass and momentum conservation. These equations are typically solved using numerical ice flow models, below referred to as *classical ice flow models*, although approximations to the full equations are often necessary due to computational constraints. Recently, alternative ways of modeling this process have emerged, relying on machine learning techniques which offer the possibility to obtain the solution at a fraction of the computational cost. Notably though, even these approaches often rely on classical ice flow models at heart. Both approaches have been used in this thesis and are described below (Table 3.1).

3.1.1 Classical ice flow models

The ice flow equations derive from the Navier-Stokes equations, the generic equations for modeling fluid flow. They are supplemented by the so-called *constitutive relationship* linking stress to strain through the material properties of ice. Specifically, ice flow can be modeled as an incompressible fluid with a high, non-Newtonian (i.e. stress dependent) and temperature dependent viscosity (Hutter, 1983; Hooke, 2005; Greve and Blatter, 2009). Due to the high viscosity, inertia terms in the Navier-Stokes equations vanish, resulting in a balance of stresses described by the Stokes equations:

Table 3.1. *Comparison of key characteristics of the two ice flow models PISM and IGM used in this thesis.*

	PISM	**IGM**
Model type	classical	physics-informed deep learning
Ice flow physics	SIA–SSA hybrid	higher-order
Discretization	finite difference	finite difference
Basal boundary condition	multiple sliding laws implemented that can be linked to subglacial hydrology model	Weertman-type sliding law
Reference	Bueler and Brown (2009)	Jouvet and Cordonnier (2023)

$$\rho \boldsymbol{g} - \boldsymbol{\nabla} p + \boldsymbol{\nabla} \cdot \boldsymbol{\tau} = \mathbf{0} \tag{3.1}$$

where ρ is the density of ice, $\boldsymbol{g}$ is gravitational acceleration, p is pressure, $\boldsymbol{\tau}$ is the deviatoric stress tensor, defined as the total stress with the isotropic pressure removed, $\boldsymbol{\nabla}$ is the gradient operator and $\boldsymbol{\nabla}\cdot$ denotes divergence. The divergence of the stress tensor represents the viscous forces per unit volume and is linked to the constitutive relationship through the ice-specific viscosity formulation:

$$\boldsymbol{\tau} \;=\; 2\,\eta\big(\dot{\epsilon}_{\mathrm{e}}(\mathbf{u})\big)\,\dot{\boldsymbol{\epsilon}}(\mathbf{u}), \qquad \eta\big(\dot{\epsilon}_{\mathrm{e}}(\mathbf{u})\big) \;=\; \tfrac{1}{2}\,A^{-1/n}\,\dot{\epsilon}_{\mathrm{e}}(\mathbf{u})^{(1-n)/n}. \tag{3.2}$$

where A is the temperature dependent rate factor, η is the effective viscosity and $\boldsymbol{u}$ denotes ice velocities. $\dot{\boldsymbol{\epsilon}}(\boldsymbol{u}) \;=\; \frac{1}{2}\big(\nabla\mathbf{u} + \nabla\mathbf{u}^T\big)$ is the strain rate tensor and $\dot{\epsilon_e} \;=\; \sqrt{\frac{1}{2}\,\dot{\boldsymbol{\epsilon}}(\mathbf{u}) : \dot{\boldsymbol{\epsilon}}(\mathbf{u})}$ is the effective strain rate, a scalar measure for the overall rate of deformation which impacts the viscosity. This viscosity formulation is referred to as Glen's flow law, with the exponent n often set to 3 and referred to as Glen's flow law exponent (Glen, 1955). Eq. (3.1) must be combined with the mass conservation equation for an incompressible fluid

$$\boldsymbol{\nabla} \cdot \boldsymbol{u} = 0. \tag{3.3}$$

Together, the Stokes equations and the incompressibility condition form a system of four equations for the three velocity components and pressure (Hutter, 1983; Hooke, 2005; Greve and Blatter, 2009). Due to the stress-dependence of the viscosity, ice near the glacier base deforms much more easily compared to higher up, resulting in a non-uniform vertical velocity profile in the ice column. Note the absence of time derivatives in the above equations, implying that glacier geometry at any instant is sufficient to accurately model

the ice flow. Conversely, this implies that in principle, bed geometry can be inferred without any time-dependent modeling.

The above system of equations is subject to boundary conditions at the glacier surface where stress-free conditions are commonly assumed. At the ice-bed interface, a boundary condition is commonly described with a friction law relating basal shear stresses to a sliding velocity. Several such laws exist which commonly assume a spatially variable parameter called friction coefficient that describes the strength of the glacier bed (Weertman, 1957; Budd et al., 1984; Schoof, 2010). When basal shear resistance is overcome, basal slip occurs, introducing a depth-independent (plug-like) velocity component at the base that alters the vertical velocity profile. The difference in how basal sliding affects the vertical velocity profile compared to viscous flow has implications for how variability in the shape of the glacier bed is transferred to the glacier surface (Raymond and Gudmundsson, 2005; Gudmundsson and Raymond, 2008). In addition, for marine- or lake-terminating glaciers, the water pressure is applied as a boundary condition at the ice-water interface (Hindmarsh, 1993).

The above ice flow equations contain several parameters that are generally difficult to constrain. These include the rate factor A which not only depends on the hard to observe englacial temperature, but also the impurity content and water fraction of the ice (Greve and Blatter, 2009). In addition, the flow law exponent, although commonly assumed to be 3, has been shown to be variable, depending on the exact form of the ice creep behavior and possible crystalline anisotropies (Behn et al., 2021; Wang et al., 2025). Moreover, the friction coefficient is generally unknown and needs to be inferred in order to constrain basal sliding (Hindmarsh, 1998). For prognostic simulations, it is often coupled to hydrological processes that determine the water availability at the glacier bed which in turn is highly correlated with the basal sliding magnitude (Bueler and van Pelt, 2015; Vallot et al., 2017).

Classical ice flow models typically solve the above equations on a discretized domain with finite difference or finite element methods. This results in model resolutions from a few tens of meters to several kilometers, depending on the computational resources available and the size of the domain (Cornford et al., 2016). A simplifying twist to domain discretization are flowline approaches, i.e. models that collapse the horizontal dimensions of the glacier into one dimension, enabling much reduced computational costs, though at the expense of missing out on possibly important across-flow variations. These models are to date the standard tool for regional and global glacier modeling studies (Maussion et al., 2019; Rounce et al., 2023). Classical ice flow models solve the ice flow equations in time steps. With higher ice flow velocities and finer grid resolution, smaller time steps need to be taken to avoid numerical instabilities (Courant et al., 1928).

A hierarchy of approximations to the Stokes equations exist that reduce computational time (Kirchner et al., 2016). Indeed, full Stokes models have

to date only been applied on individual glaciers (e.g. Jouvet et al., 2008) or in a few cases on an ice-sheet wide scale (e.g. Karlsson et al., 2021) due to the computational costs. Each of the approximations comes with certain assumptions on the dominant ice flow process and the relative magnitude of certain geometric properties of the modeled glacier (Kirchner et al., 2016).

Leading-order shallow approximations include the shallow ice approximation (SIA) and the shallow shelf approximation (SSA). The SIA neglects horizontal stress gradients, implying that ice flow is entirely local and downhill, with the solution for surface velocities being obtainable through a vertically integrated formulation that removes the need for vertical discretization of the ice column. The key assumption at the heart of the SIA is a small aspect ratio of the glacier, with the horizontal length scale being much larger than the ice thickness (Hutter, 1981). This is typically true in the interior of ice sheets and large ice caps, for which this approximation was developed, while being less applicable on mountain glaciers. To approximate the effects of the otherwise neglected longitudinal stress gradients, smoothing of the basal shear stress over a so-called longitudinal coupling length can be done, the latter being on the order of a few times the ice thickness (Kamb and Echelmeyer, 1986).

Like the SIA, the SSA is vertically integrated, with the key approximation being the neglect of vertical normal and shear stress gradients (Morland, 1987; MacAyeal, 1989). This assumes plug flow with a vertically uniform ice flow profile, as obtained when sliding dominates over internal deformation. Typical settings include ice shelves and fast-flowing outlet glaciers. The SSA is non-local, implying that distant locations can influence the ice flow velocity at a given point. Both the SSA and the SIA are computationally cheap as compared to all other approximations. Ice flow models relying on the SIA or SSA or a combination thereof include the Open Global Glacier Model (OGGM; Maussion et al., 2019) and the Parallel Ice Sheet Model (PISM; Table 3.1; Bueler and Brown, 2009).

There exist several higher-order approximations, the most widely used being the Blatter-Pattyn approximation (Blatter, 1995; Pattyn, 2003). It neglects horizontal gradients of the vertical normal stress while retaining vertical and horizontal shear stress gradients. This makes it more suitable for mountain glaciers where the SIA and SSA assumptions are not met. Higher-order models increase computational demand significantly compared to the shallow approximations, while still being considerably cheaper than full Stokes models (Zekollari et al., 2022). The error introduced by relying on approximations rather than the full Stokes equations depend on the specific set up. While several studies show that the time-integrated glacier response in long-term simulations of glacier retreat is similar between a full Stokes and a SIA model (Åkesson et al., 2017; Zekollari et al., 2022), the instantaneous velocity solution may differ significantly in diagnostic stress balance or short-term simulations (Adhikari and Marshall, 2013).

3.1.2 Machine-learning ice flow models

The high computational demands of higher-order and full Stokes models have proven to be a bottleneck for accurate decennial to centennial glacier simulations on large scales, such as in global glacier modeling (Seroussi et al., 2020; Zekollari et al., 2025), for paleo-ice sheet simulations (Leger et al., 2025) or for ice sheet projections, as well as for inversion problems, model calibration and uncertainty quantification (Brinkerhoff et al., 2016, 2021; Aschwanden and Brinkerhoff, 2022). To overcome these computational limitations, machine learning approaches have increasingly been explored as fast statistical emulators of ice flow models (Bolibar et al., 2023). Machine learning refers to algorithms that improve their performance on a task by optimizing parameters based on data rather than being explicitly programmed (Bishop and Nasrabadi, 2006). Deep learning is a branch of machine learning where this mapping is represented by Artificial Neural Networks (ANNs) composed of many interconnected layers (LeCun et al., 2015; Goodfellow et al., 2016). Each layer applies a transformation to its inputs: connections between layers carry weights (the trainable parameters of the network), and nonlinear activation functions are applied to allow the network to approximate complex, nonlinear relationships. During training, the network adjusts its weights through optimization algorithms (e.g. stochastic gradient descent) which minimize a loss function that measures prediction error. This structure allows neural networks to learn rich input–output relationships from data (LeCun et al., 2015; Goodfellow et al., 2016). Recent advancements in such methods have sparked the development of statistical ice flow model emulators that implicitly learn the underlying ice flow equations during training and are computationally cheap when evaluated (Fig. 3.1; Bolibar et al., 2023). The rationale is to find a statistical mapping from input data (e.g. ice thickness, surface slope, basal conditions) to ice flow model output (typically velocities), a task for which ice flow problems exhibit several favorable properties, in particular the time-independence of the Stokes equations and the typically slow evolution of glacier geometry (Jouvet et al., 2022).

Inspired by previous applications in fluid dynamics and (non-ice dynamics) glaciology (Clarke et al., 2009; Bolibar et al., 2020), this work was pioneered by Brinkerhoff et al. (2021) who employed an ANN to emulate the solution of a computationally demanding coupled ice dynamics - subglacial hydrology model in order to enable Markov Chain Monte Carlo calibration of model parameters. Other notable works include He et al. (2023) with a finite-element based deep neural operator and Jouvet et al. (2022) using a Convolutional Neural Network (CNN). The overall principle of these approaches is the same, and falls into the category of supervised learning: first, a high-fidelity physical ice flow model is run in different configurations that are thought to span the 'envelope' of all future applications of the emulator. This is important to consider as machine learning tools generally are good interpolators, but not suited for ex-

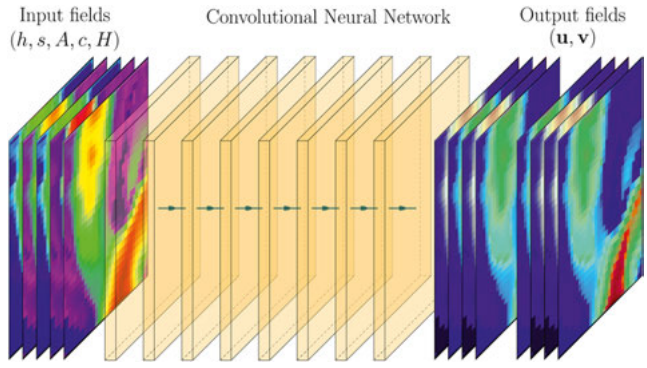

Figure 3.1. Schematic of an ice flow model emulator. Given a set of input fields, a multi-layer Convolutional Neural Network (or comparable other machine learning architecture) is trained to predict the output (often ice flow velocities) of a physical ice flow model. Source: Jouvet and Cordonnier (2023).

trapolation (Bishop and Nasrabadi, 2006). Subsequently, the machine learning model is trained, with different machine learning architectures being suitable for different setups: for finite-difference physical models, CNNs have emerged as powerful tools as they directly consider spatial relationships between grid cells through convolution operations, thus preserving non-local features of the ice flow (Jouvet et al., 2022). Meanwhile, for finite-element physical models, Graph Neural Networks (GNNs) are a natural option (He et al., 2023; Koo and Rahnemoonfar, 2025) as they natively consider the underlying unstructured mesh. The computational gains obtained with machine learning emulators are considerable, partly also due to their ability to run in a massively parallelized manner on Graphic Processing Units (GPUs): Jouvet et al. (2022) report computational speed-ups with a factor 1000, while Koo and Rahnemoonfar (2025) indicate this number to be 60-100. Note though that this is during evaluation of the models; the generation of training data remains a costly task under supervised learning (LeCun et al., 2015; Goodfellow et al., 2016).

Whereas Brinkerhoff et al. (2021); He et al. (2023); Koo and Rahnemoonfar (2025) trained their emulators for one glacier or region specifically, Jouvet et al. (2022) were the first to propose a general model, called Instructed Glacier Model (IGM), that could be applied in various settings. This was achieved by training IGM on a catalog of four ice fields previously simulated with PISM (Bueler and Brown, 2009) and, separately, 41 mountain glaciers simulated with a full Stokes model (Jouvet et al., 2008). The basal topography for the simulations was taken from real-world deglaciated mountains. The CNN was trained with the same inputs given to the physical ice dynamics models (ice thickness, surface slope and a basal friction field) as well as with the output depth-integrated velocity fields. Validation on glaciers unseen during training showed high fidelity scores, despite the size of the CNN as measured by its number of trainable parameters being relatively small (65,000 and 140,000 for

the ice field and the mountain glacier model, respectively; modern large language models have several orders of magnitudes more (Walker, 2024)). Nevertheless, the wider applicability of IGM as presented in Jouvet et al. (2022) was hampered by constraints inherent to the model structure and training: glaciers outside the envelope of the training data could not be simulated and grid resolution was limited to that which the model was trained on, as were values for the ice viscosity.

To overcome such limitations, physics-informed neural network (PINN) emulators have become promising tools (Jouvet and Cordonnier, 2023; Cheng et al., 2024, 2025; Wang et al., 2025). In contrast to the previously described machine-learning architectures they directly integrate physical constraints into the model. This is done by modifying the loss-function to include ice flow physics. That is, the emulator should not only provide a solution that appears similar to the one from the physical model, but the solution should also adhere to certain physical constraints. As such, the machine-learning model is not only based on the training data supplied by an instructor model, but has an internal constraint forcing it to stay close to a physical solution. This has proven particularly useful in inversion contexts where a data loss (i.e. a model solution - observational data misfit) and an equation loss (i.e. a model solution - physics misfit) can be combined to a total loss (Cheng et al., 2024; Wang et al., 2025; Cheng et al., 2025). During training, the underlying machine-learning model aims to minimize both, ensuring that an output is produced that is tightly constrained by known though imperfect model physics and the available observations. This circumvents the often encountered dependency on rigid physical models with poorly constrained parameters while at the same time being able to account for errors in observational data. Based on the weights given to the data loss and the equation loss, a tradeoff can be made between relying more on the physical model vs. placing more trust in the data (Cheng et al., 2024; Wang et al., 2025; Cheng et al., 2025).

To generalize their machine-learning emulator IGM using physics-informed deep learning (Table 3.1), Jouvet and Cordonnier (2023) adopted an approach inspired by variational physics-informed neural networks (VPINNs). Unlike standard supervised training, this method removes most of the need for pre-generated training data from a costly physical model. VPINNs do not fit data directly but instead rely on the variational (minimization) form of the governing physical equations. In practice, Jouvet and Cordonnier (2023) reformulated the higher-order ice-flow equations so that they express the energy of the ice-flow system, with the physically consistent solution corresponding to the velocities that minimize the energy functional (Jouvet and Cordonnier, 2023):

$$J(\mathbf{v}) = \int_V 2\frac{A^{-1/n}}{1+1/n}\,\dot{\epsilon}_{\mathrm{e}}(\mathbf{v})^{\,1+1/n}\,dV + \int_{\Gamma_b} \frac{c^{-m}}{1+m}\,|\mathbf{v}|^{\,1+m}\,dS + \rho g \int_V (\nabla s \cdot \mathbf{v})\,dV \tag{3.4}$$

where the first term on the right hand side represents the constitutive relationship with V being ice volume, the second term a Weertman-type sliding law with an exponent m and a friction coefficient c applied along the basal boundary Γ_b and the last term the gravitational forces where s is the glacier surface. Here, $\mathbf{v}$ represents a trial or candidate velocity field, which is varied during minimization until the physically consistent solution $\boldsymbol{u}$ is obtained. Note that for the calculation of the strain rate tensor, horizontal gradients of the vertical normal stresses are neglected in line with the higher-order approximation (Blatter, 1995). The minimization is carried out using automatic differentiation and stochastic gradient methods, and the performance of this solver was validated against standard benchmark cases. Building on this, the authors then integrated a CNN. Starting from the pre-trained CNN from the "old" IGM (Jouvet et al., 2022), its weights can be updated transiently during model runs so that the CNN predictions also minimize the energy of the system. Each such "retraining" step consists of a forward pass through the CNN (producing a first velocity prediction), followed by a calculation of the system energy and its gradients. These gradients are then used to update the CNN weights, so that in future passes the CNN-predicted velocities move closer to the energy-minimizing solution that the solver would otherwise compute. Conveniently, this allows the computationally expensive solver to be run only intermittently, while the CNN can provide inexpensive emulated solutions between solver calls. With each retraining step, the CNN is nudged toward the physically correct solution, enabling applications that are independent of pre-generated training data. This physics-informed version of IGM has now become a widely used model (e.g. Cook et al., 2023b; Kneib et al., 2024; Leger et al., 2025), with the previous version (Jouvet et al., 2022) being no longer maintained.

3.2 Ice thickness inversion problems

Estimating the unknown bed topography and ice thickness from surface observations is often referred to as an inversion. Note that the terms bed inversion and ice thickness inversion are used interchangeably below as bed elevation and thickness may be regarded as equivalent given knowledge of the surface height. In a general sense, an inversion problem may be described as map-

ping observed data to an estimate of the unknown quantity via a model of the governing process

$$\boldsymbol{d} \rightarrow f(\boldsymbol{m}) \tag{3.5}$$

where f represents the model, $\boldsymbol{m}$ are the model parameters, including the unknown, and $\boldsymbol{d}$ is observed data. In a glaciological bed inversion context, f is an ice-flow model, $\boldsymbol{m}$ are its parameters, such as the rate factor A, the surface topography s and the bed topography b, while $\boldsymbol{d}$ can include observations of ice flow velocities or rate of surface elevation change. Inversion methods have a long tradition in glaciology, in particular, to constrain the friction coefficient (MacAyeal, 1992, 1993), but this chapter will focus specifically on ice thickness inversions.

A classical way of addressing inversion problems in fluid dynamics is through variational methods where a misfit or cost function $J(\boldsymbol{m})$ between an observed quantity and model output is defined, e.g.

$$J(\boldsymbol{m}) = ||\boldsymbol{d} - f(\boldsymbol{m})|| + ... \tag{3.6}$$

that is minimized through an iterative process, where the three dots indicate that additional terms can be included in the misfit function (Goldberg and Heimbach, 2013; Morlighem et al., 2017; Jouvet, 2023). For bed inversions, these may include terms enforcing smoothness of the solution or penalties for non-zero ice thicknesses outside defined glacier outlines. Additional terms may also be included to infer several parameters simultaneously, although this requires a corresponding number of observational datasets to avoid underdetermined problems (Goldberg and Heimbach, 2013). Iterations are necessary when the underlying model is non-linear and complex, as is the case for non-local ice flow models. The critical question then is how to find the model parameters for the next iteration that yield a reduction in the misfit. This can be expressed as finding the derivative of the cost function with respect to the parameters, i.e.

$$\nabla_{\boldsymbol{m}} J(\boldsymbol{m}) \; = \; \frac{\partial J}{\partial \boldsymbol{m}} = \frac{\partial J}{\partial f} \, \frac{\partial f}{\partial \boldsymbol{m}}, \tag{3.7}$$

obtained from applying the chain rule to Eq. (3.6). A naive trial-and-error search is intractable considering the high number of unknowns (e.g. the thousands of grid points of a bed topography map) and is furthermore unlikely to result in an identification of the global minimum (MacAyeal, 1993). Instead, these gradients are often calculated using an adjoint model, i.e. a "backward" model yielding the gradients of the cost function with respect to the model parameters (e.g. Morlighem et al., 2017). However, the derivation of the adjoint is complex, in particular for more sophisticated (coupled) models (Cheng et al., 2025). Furthermore, adjoint-based inversion is susceptible to getting

stuck in local minima of J, and adjoint model evaluation is computationally expensive (Goldberg and Heimbach, 2013; Jouvet, 2023). Recent advancements may alleviate some of these issues and are increasingly explored, though their large-scale applicability remains to be proven. These include tools for automatically generating fully differentiable code (Bezanson et al., 2017; Bolibar et al., 2023; Utkin et al., 2025), summarized under the term Automatic Differentiation, such as the programming language Julia (Bezanson et al., 2017). In addition, machine learning tools offer exciting possibilities as they are both fully differentiable by design and allow to reduce computational demands of the process model (Sec. 3.1.2). Jouvet (2023) was the first to explore this using an early version of IGM. This was subsequently exploited on a regional scale by Cook et al. (2023b) for all glaciers in the Alps.

A related, though different, approach is to iteratively improve the estimate of the unknown via "heuristic" gradients that emerge directly from the nature of the problem (Heining, 2011; Michel et al., 2013; van Pelt et al., 2013). Instead of calculating the direct cost function gradient as in Eq. (3.7), such an approach improves the guess of the unknown directly from comparing model output with observations. An example of that is van Pelt et al. (2013) where point-wise iterative updates to the bed topography B are applied as a function of the misfit between modeled (mod) and observed (obs) surface elevations following

$$B^{i+1} = B^i - \left(s^i_{\text{mod}} - s_{\text{obs}}\right) \tag{3.8}$$

with i as the iteration count. The associated cost function gradient

$$\nabla_B F = \frac{\partial F}{\partial s_{\text{mod}}} \frac{\partial s_{\text{mod}}}{\partial B} = \frac{\partial F}{\partial s_{\text{mod}}} I = s_{\text{mod}} - s_{\text{obs}} \tag{3.9}$$

is equivalent to Eq. (3.7) but assuming that the Jacobian $\frac{\partial s_{\text{mod}}}{\partial B}$, i.e. the derivative of the surface elevation with respect to bed elevation, is the identity matrix I (i.e. a square matrix with ones on the diagonal). Such an approach was previously shown by Heining (2011) to work for gravity-driven, viscous flows, and a further development of the van Pelt et al. (2013) method was used extensively in this thesis. It avoids the need to derive complex adjoint models, enabling relatively straightforward applications even for complex, possibly coupled models, including full Stokes ones. It also renders the inversion process generally robust and easy to interpret as the evolution of the misfit can directly be linked to the process simulated. However, the "descent path" of this method from the initial guess towards the final solution may be less stringent compared to using a method that calculates the full cost function gradients $\nabla_{\boldsymbol{m}} J(\boldsymbol{m})$ including the Jacobian. Furthermore, including additional or non-local terms in the misfit is not straight-forward. For example, in Eq. 3.8, a penalty on non-zero ice thickness outside observed glacier outlines is not naturally enforced: the update rule acts locally at each grid cell (due to the model Jacobian being assumed to be the identity matrix) and therefore does not, by itself, exploit the model's long-range sensitivities. This is different from adjoint-

or Jacobian-based methods which calculate the sensitivity of the model output (e.g. surface height) at any location to the input (e.g. bed elevation) at any location, allowing to establish a cost function gradient that can take into account how far-apart grid cells affect each other (MacAyeal, 1993).

In contrast to iterative inversion methods, the local SIA allows direct inversions in one step due to its simple algebraic nature. Specifically, the SIA can be written as

$$h = \left(\frac{(u_s - u_b)(n+1)}{2A(\rho g \nabla s)^n} \right)^{\frac{1}{n+1}} \tag{3.10}$$

to relate ice thickness and observed surface velocities (Millan et al., 2022), provided an estimate on the sliding velocity u_b, or similarly

$$h = \left(\frac{\bar{q}(n+2)}{2A(\rho g \nabla s)^n} \right)^{\frac{1}{n+2}} \tag{3.11}$$

to relate the thickness to the depth-integrated ice flux $\bar{q}$ which can be estimated from observations of surface mass balance and surface elevation change (Farinotti et al., 2009). This has large computational advantages compared to more complex approaches. Consequently, this method has seen wide applications for glacier inversions (e.g. Farinotti et al., 2009; Huss and Farinotti, 2012; Gantayat et al., 2014; Maussion et al., 2019), including to produce the currently available global ice thickness products (Farinotti et al., 2019a; Millan et al., 2022). However, the output thickness absorb all the errors from the insufficient SIA model physics, implying that the bed may exhibit characteristics that are irreconcilable with our full understanding of ice flow dynamics. The same is true for perfect-plasticity approaches (Nye, 1951; Linsbauer et al., 2012; Frey et al., 2014) which equally reduce the ice-flow physics to an algebraic equation which can be solved directly for ice thickness. This requires making an assumption on the basal yield stress, a property generally poorly constrained.

Further inversion approaches exist and have been applied in the glaciological literature. This includes Bayesian inversions (Brinkerhoff et al., 2016; Morin et al., 2023) that pose the problem in a probabilistic framework. Time-dependent inversions are also becoming increasingly popular thanks to their ability to assimilate observations collected over longer periods, thus enhancing the observational datasets that can be exploited (Goldberg and Heimbach, 2013; Utkin et al., 2025). Another way of inferring glacier beds is through geostatistical methods such as kriging, although this is rather an interpolation method between radar observations than an inversion (Kitanidis, 1997; Neven et al., 2021; Vanlooy et al., 2014). None of these approaches have so-far been applied on large scales, either due to computational costs or insufficient input data.

Ice thickness inversions are ill-posed problems in that they are non-unique, i.e. theoretically, an infinite number of solutions can explain the observations, and sensitive to the input data, i.e. small changes in the observations may result in large changes in the recovered bed (Bahr et al., 2014; Habermann et al., 2012). These properties arise directly from the ice flow equations. The viscous deformation of ice implies that variability in the basal topography is transferred to the glaciers surface in a much damped way (Gudmundsson, 2003; Raymond and Gudmundsson, 2005; Gudmundsson and Raymond, 2008). In other words, the glacier surface shape is a low-pass filtered representation of the bed. This loss of detail implies that when recovering the bed from surface shape information, no statement can be made on the existence or non-existence of high-frequency basal variability (Habermann et al., 2012). At the same time, any feature visible on the surface represents a much larger feature on the bed, explaining why small errors in a surface elevation dataset would result in much larger errors in the recovered bed. The degree to which basal variability is transferred to the surface depends on the geometry of a given basal feature, the surface slope and the ratio between deformation and sliding (Gudmundsson, 2003; Raymond and Gudmundsson, 2005). Whereas features with a horizontal extent below about one time the ice thickness do not leave any surface expression in deformation dominated flow, and consequently cannot be recovered with inversion methods, features beyond that are increasingly reproduced on the surface, with full similarity of bed and surface undulations reached for bed features with a horizontal extent greater than 70 times the ice thickness. With sliding dominated flow, basal features are much more readily reproduced at the surface due to basal slip affecting the entire ice column uniformly, in contrast to deformational flow (Morin et al., 2023). However, even so small scale features leave no surface expression (Raymond and Gudmundsson, 2005), implying that the spatial resolution of thickness datasets must be critically evaluated against the local ice thickness.

To avoid producing beds with high-frequency undulations that are not justified by the surface observations requires to bias the inversion towards such outcomes (Habermann et al., 2012). This is called regularization. In variational approaches, regularization is often done by including terms in the misfit functional that penalize strong gradients in the thickness field (Fürst et al., 2017; Jouvet, 2023). Other approaches implicitly regularize through stopping the inversion before small-scale features are produced (van Pelt et al., 2013) or by smoothing input data (Farinotti et al., 2009).

Thickness inversions in glaciology often rely either on a mass conservation principle or on observed velocities, with some approaches also combining the two (Farinotti et al., 2017, 2021). An important difference between them is that velocity-based approaches are time-independent as they only rely on the stress balance equations which yield a velocity solution from the geometry of the glacier alone (Jouvet, 2023). In theory, this may be considered the most logical approach to ice thickness inversion with the advantage that the required

velocity observations are obtainable from space and generally subject to little inter-annual variability. This was exploited by Millan et al. (2022) to produce a global map of ice thicknesses, though using the SIA following Eq. (3.10). Cook et al. (2023b) employed IGM on all glaciers in the Alps in a velocity-based approach with variational methods. However, noise often found in velocity observations poses a challenge. In addition, such approaches are not ideally suited for ensuing prognostic modeling as they often yield a thickness field which is not aligned with the mass balance forcing, causing strong artificial initial changes to the glacier geometry in forward simulations (Zekollari et al., 2022).

Mass conservation approaches do not suffer from these issues as they integrate mass balance observations or model output during the inversion (Farinotti et al., 2009; Morlighem et al., 2011). They are typically based on a two-dimensional form of the mass continuity equation which in a glaciological context can be written as

$$\frac{\partial h}{\partial t} + \nabla \cdot h\bar{\boldsymbol{u}} = \dot{b} \tag{3.12}$$

where $\dot{b}$ is the specific climatic mass balance, i.e. the positive or negative sum of all mass fluxes at a given point over one year (Morlighem et al., 2011). Eq. (3.12) states that the flux divergence $\nabla \cdot h\bar{\boldsymbol{u}}$ must be balanced by the climatic mass balance or ice thickness changes. By knowledge of the latter two (with $\frac{\partial h}{\partial t}$ and $\dot{b}$ being observable at the surface) and through modeling the depth-averaged velocities $\bar{\boldsymbol{u}}$, the ice thickness is inferred. Example applications of this approach include the global ice thickness study by (Farinotti et al., 2019a) and the inversion method used in OGGM (Maussion et al., 2019). The widely used BedMachine bed products for Greenland (Morlighem et al., 2017) and Antarctica (Morlighem et al., 2020) are generated using both velocity observations and mass balance, though in the way that their functional principle is closer to mass conservation approaches, yet using observed velocities in Eq. (3.12). This removes the need for an ice-flow model and makes these products strongly observation-based.

Different inversion methods also differ in their ability to assimilate observations of ice thickness where they exist (Farinotti et al., 2021). Variational approaches can include a term penalizing mismatches between modeled and observed thicknesses such that they naturally profit from the observations even away from observed locations (Morlighem et al., 2011; Jouvet, 2023; Cheng et al., 2024). By contrast, methods that do not involve computing the Jacobian or the adjoint model need to rely on more ad-hoc methods to achieve a match with observations, with the information gain for unobserved locations being less clear. An example of that is Fürst et al. (2017, 2018, 2024); Shahateet et al. (2025) who calculated the ice viscosity where the ice thickness is known and subsequently interpolated those values in space. While this ensures

a perfect thickness match at observed locations, the spatial interpolation is not constrained by a physical understanding of ice viscosity variability.

3.3 Large-scale glacier modeling

A specific subdiscipline of glacier modeling concerns large-scale applications. Here, this refers to applications of glacier models on regional to global scales, often encompassing thousands to hundred thousands of glaciers (e.g. Radić and Hock, 2010; Marzeion et al., 2012; Farinotti et al., 2019a; Rounce et al., 2023; Zekollari et al., 2025; Schuster et al., 2025). Large-scale glacier modeling may be done either to infer glacier properties (e.g. global ice volume; Radić and Hock, 2010; Grinsted, 2013; Farinotti et al., 2019a; Millan et al., 2022) or to project the future evolution of a large sample of glaciers (e.g. Marzeion et al., 2012; Rounce et al., 2023; Zekollari et al., 2025; Schuster et al., 2025). The large-scale perspective brings specific challenges related to input data, computational constraints and interpretation of the output. The need for such studies is evident from the observed large-scale retreat of glaciers: while the impact of one glacier's mass loss is mostly local, it is the combined response of all glaciers in a region or on the globe that alters Earth system processes on a wide scale, e.g. by raising sea levels (IPCC, 2021).

Explicitly modeling every single glacier on Earth was long considered impossible. Statistical theories were sought instead that would explain the mean behavior of a sample of glaciers with each individual glacier showing a random deviation from that. A prominent example of such an approach is Volume-Area scaling which assumes a fixed relationship between the (easily observable) glacier area and its volume (Bahr et al., 1997). This method has been used repeatedly to estimate global glacier volumes, e.g. Raper and Braithwaite (2005); Grinsted (2013); Radić et al. (2014). Volume-Area scaling has also been used to represent the ice dynamics in future simulations (Radić and Hock, 2011; Marzeion et al., 2012), a strong simplification which, for instance, disregards feedbacks from changes in surface elevation (Radić and Hock, 2014). Statistical methods related to mass balance modeling in global-scale studies include extrapolation of observation from a few hundred to all glaciers (Dyurgerov and Meier, 1997; Ohmura, 2004). The key limitation here is the small and uneven global availability of glacier observations, with most observations concentrated in Europe and North America, and their known unrepresentativeness of the regional or global glacier population (Zemp et al., 2025).

Large-scale glacier models then became increasingly complex regarding both the computation of mass balance and ice dynamics (Radić and Hock, 2014). To compute the former, models focused on temperature and precipitation based approaches where the two inputs were obtained from global climate models (e.g. Marzeion et al., 2012; Radić et al., 2014). This allows to force the mass balance models with ensembles of climate models such as obtained from

the Climate Model Intercomparison Project (Meehl et al., 2000) , which in return results in ensembles of mass balance projections. Increasingly, models have also included the effect of debris cover on mass balance (Rounce et al., 2021, 2023) as well as explicitly modeling frontal ablation (Maussion et al., 2019; Recinos et al., 2021; Rounce et al., 2023). Key challenges for large-scale temperature and precipitation based models remain the high spatial variability of these variables in mountainous terrain in conjunction with the coarse resolution of the climate models (Zekollari et al., 2022, 2024). In addition, small-scale mass balance processes that may be very important for individual glaciers are generally neglected or poorly represented, such as avalanching (Kneib et al., 2024), snow drift (Terleth et al., 2023), refreezing (van Pelt et al., 2019) or basal melting (Magnússon et al., 2005). Meanwhile, transitioning to full energy balance models has so far proven challenging given that such approaches are very sensitive to an accurate representation of the individual energy balance components (e.g. shortwave radiation, albedo, longwave radiation) which are generally not well enough represented in global climate models (Radić and Hock, 2014; Zekollari et al., 2022).

Regarding ice dynamics, large-scale models have transitioned from the simplistic approaches described above to process-based models based on the SIA (Maussion et al., 2019; Rounce et al., 2023). A few models also use the so-called Δh parameterization which is an empirical function that calculates the typical surface elevation change resulting from changes in ice dynamics as glaciers retreat (Huss et al., 2010; Huss and Hock, 2015). Notably, large-scale ice dynamics models to date rely on flowline approaches which reduce computational demand and simplify the calculations (Huss and Hock, 2015; Maussion et al., 2019; Rounce et al., 2023). Although SIA-based flowline models are a clear improvement compared to earlier approaches, they remain highly simplified representations of the ice flow physics. One large-scale study forming an exception to such approaches is Cook et al. (2023b) who modeled committed mass loss in the Alps using IGM (Jouvet et al., 2022) on a distributed grid.

Large-scale glacier models rely on input data with large, often global, coverage to produce spatially consistent results. These will be discussed in more detail in the next chapter as they were also used in this thesis. Such datasets often come with elevated uncertainties relative to local products (Zemp et al., 2025).

Recent focus has increasingly turned towards initialization of glacier models through data assimilation techniques using observations from the recent past (Cook et al., 2023a; Herrmann et al., 2025; Schmitt et al., 2025). This trend is due to several studies showing the importance of initialization for near-term glacier projections (Hock et al., 2019; Cook et al., 2023b; Schuster et al., 2023; Zekollari et al., 2024). However, glacier models still tend to be overparameterized in that they have a large number of parameters relative to the number of available observations, implying that poorly constrained parameters remain (Felikson et al., 2025). To address this challenge, assumptions are made where

possible, e.g. by tuning a uniform ice viscosity value for all glaciers in a region (Farinotti et al., 2019a; Millan et al., 2022; Rounce et al., 2023). This contributes to elevated parametric uncertainty of large-scale models compared to local studies that can perform more targeted tuning.

Although large-scale glacier modeling today has moved away from statistical approaches and turned towards explicitly modeling every single glacier on Earth, there remain important limitations that need to be considered when interpreting the results of such studies (Hock et al., 2019; Zekollari et al., 2024). Specifically, uncertainties for any individual glacier are much higher compared to a dedicated small-scale study due to 1) mass balance calculations chiefly based on temperature and precipitation output from coarse-resolution climate models, 2) highly simplified ice dynamics based on the SIA and applied along flowlines, 3) large-scale input data that may exhibit considerable uncertainty for an individual glacier and 4) increased parametric uncertainty resulting from overparameterized models. Thanks to increasingly rigorous calibration strategies and increasingly complex models, the bulk behavior of glaciers modeled in large-scale studies can generally be assumed accurate, but deviations on a local scale are to be expected (Hock et al., 2019; Zekollari et al., 2024). This is true for both large-scale inversion studies and future projections.

Nordenskiöldbreen
Svalbard

Photo: Thomas Frank

4. Methods and Data

Given the simplifications in large-scale bed inversion studies described above, in particular the reliance on SIA-based flowline models, this thesis work identified the need to develop a novel thickness inversion method which produces bed elevations that better reflect our physical understanding of ice flow while being robust and computationally affordable at large scales. Since the developed method is at the heart of the entire thesis work, it will already be presented here while the Summary of papers chapter later will focus on presenting specific applications. These applications of the method on regional and global scales required large-scale input data products which will also be presented briefly below.

4.1 A novel thickness inversion method

The glacier thickness inversion method is formulated as an iterative optimization problem, aiming to identify the bed topography and basal friction field that best reproduce the observed dynamic state of a glacier under known boundary conditions (Fig. 4.1, 4.2). It follows from the inverse method proposed by van Pelt et al. (2013) (Eq. (3.8)) but removes the need for long time-dependent simulations. In the context of inverse problems, this corresponds to minimizing a misfit functional between modeled and observed quantities that are sensitive to the unknown parameters — in this case, the bed elevation and basal friction.

Starting from an initial estimate of the bed topography B, the ice flow model is forced with the observed surface elevation, the climatic mass balance field, and an initial guess for basal friction. The model is integrated forward over a short time step to compute the modeled rate of surface elevation change, $(dh/dt)_{\text{mod}}$. This field is compared to the observed rate $(dh/dt)_{\text{obs}}$, and the bed is updated according to

$$B^{i+1} = B^i - \beta \left(\frac{dh^i_{\text{mod}}}{dt} - \frac{dh_{\text{obs}}}{dt} \right), \tag{4.1}$$

where β is a relaxation parameter that controls the amplitude of the bed correction (Fig. 4.1). Conceptually, this step modifies the bed in the direction that reduces the local imbalance between the modeled and observed vertical flux divergence, thereby following a mass conservation approach. The process is repeated iteratively until the misfit between $(dh/dt)_{\text{mod}}$ and $(dh/dt)_{\text{obs}}$ is resolved.

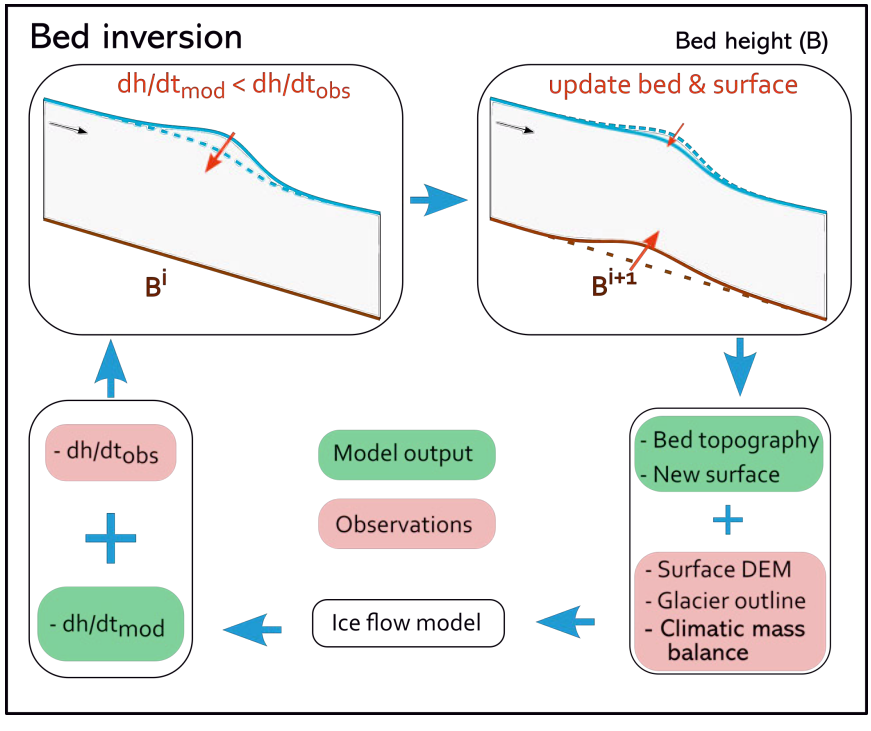

Figure 4.1. Sketch of the iterative bed inversion process. Using observations of surface height, glacier outlines and climatic mass balance, an ice flow model is ran iteratively and bed heights B are updated based on the misfit between modeled and observed dh/dt according to Eq. (4.1). A corresponding surface change is applied following Eq. (4.2).

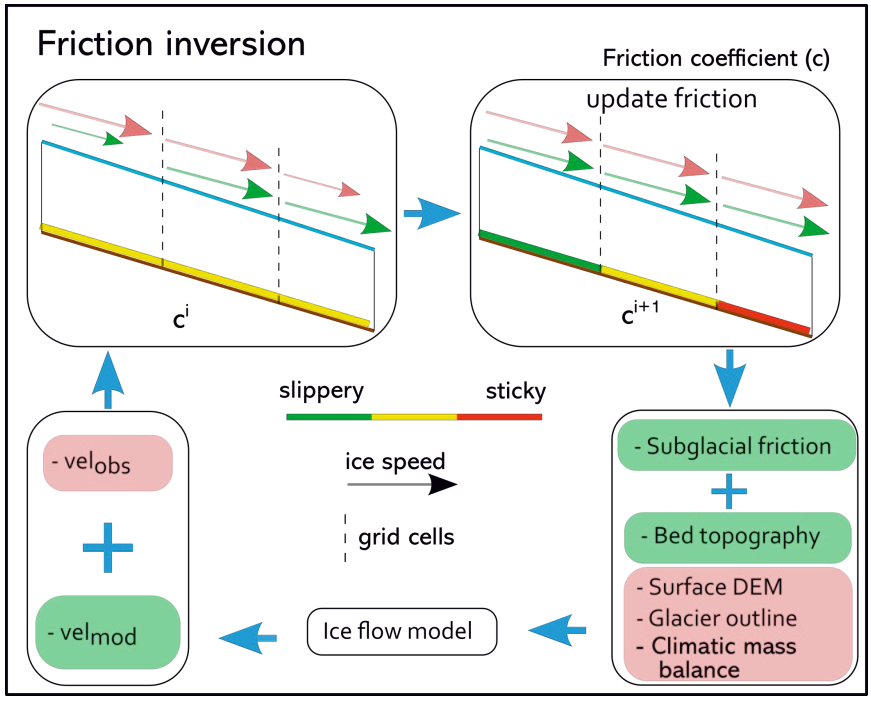

Figure 4.2. Sketch of the iterative friction inversion process. Following the same logic as in Fig. 4.1 friction c is updated pointwise according to Eq. (4.3) based on the misfit between modeled and observed velocities.

Because bed inversion problems are ill-posed and non-unique, regularization is introduced to suppress unrealistic small-scale oscillations in the recovered bed. This is achieved by coupling each bed correction to a small, oppositely directed surface correction,

$$S^{i+1} = S^i + \theta\beta \left(\frac{dh^i_{\text{mod}}}{dt} - \frac{dh_{\text{obs}}}{dt} \right), \tag{4.2}$$

where $\theta \ll 1$ determines the fraction of the bed update applied to the surface. These surface adjustments redistribute the driving stress, allowing the system to accommodate residual inconsistencies (e.g., in mass balance forcing or model physics) through minor changes in surface elevation rather than through exaggerated bed modifications.

In regions where basal sliding exerts a significant control on ice dynamics, the inversion is extended to simultaneously recover the spatially variable basal friction coefficient c. The goal is to minimize the mismatch between modeled and observed surface velocities, u_{mod} and u_{obs}, respectively. The friction field is therefore iteratively updated following a correction rule of the form:

$$c^{i+1} = c^i \times \left(1 + F\left(\frac{u^i_{\text{mod}} - u_{\text{obs}}}{u_{\text{obs}}}\right)\right), \tag{4.3}$$

where $F(x) = \min(\max(x, -\lambda), \lambda)$, $\lambda = 0.8$ is a bounded function that limits the amplitude of updates to prevent overcorrections (Fig. 4.2).

Because both the bed and friction field influence the same modeled quantities, they are not updated simultaneously. Instead, several bed iterations are performed for a fixed friction field until convergence in dh/dt is achieved, after which the friction field is updated once based on the velocity misfit. This alternating inversion ensures that the model sequentially satisfies both the surface-elevation-change and surface-velocity constraints.

From an inversion-theoretical perspective, the method can be viewed as a fixed-point iteration for minimizing a cost functional that quantifies the misfit between modeled and observed glacier dynamics, regularized by smoothness constraints on the unknown fields. It belongs to the class of "heuristic" gradient-descent-type methods as described in Sec. 3.2, where the direction of parameter updates is proportional to the local sensitivity of the misfit function to the unknowns. Rather than computing explicit derivatives, the updates are constructed from physically motivated correction rules derived directly from the ice flow equations. As such, the model Jacobian is not explicitly calculated but assumed to be the identity matrix. Although a simplification compared to adjoint-based inversions, this renders the inversion robust and Heining (2011) showed that such an inversion converges to the solution for viscous gravity-driven flows.

The inversion leverages the forward ice flow model as a physical operator linking the unknown parameters (bed and friction) to the observable quantities (surface geometry, velocity, and dh/dt). Through successive corrections, the model converges to a dynamically consistent configuration that explains the observed non-steady glacier behavior while maintaining physically plausible smoothness and stability properties. As the final thickness field is consistent with the model physics and the input data, the inversion method yields a spun-up glacier state that can be run into the future without further relaxation, provided that the exact same model configuration is used.

4.2 Global and regional datasets

4.2.1 Glacier outlines

At the heart of each regional or global glacier study is an inventory of glacier outlines which define the modeling domain. The Randolph Glacier Inventory (RGI; Pfeffer et al., 2014; RGI Consortium, 2017) is such a community-compiled, globally complete digital compilation of glacier outlines assembled to provide a standardized snapshot of glacier extents at the turn of the 21st

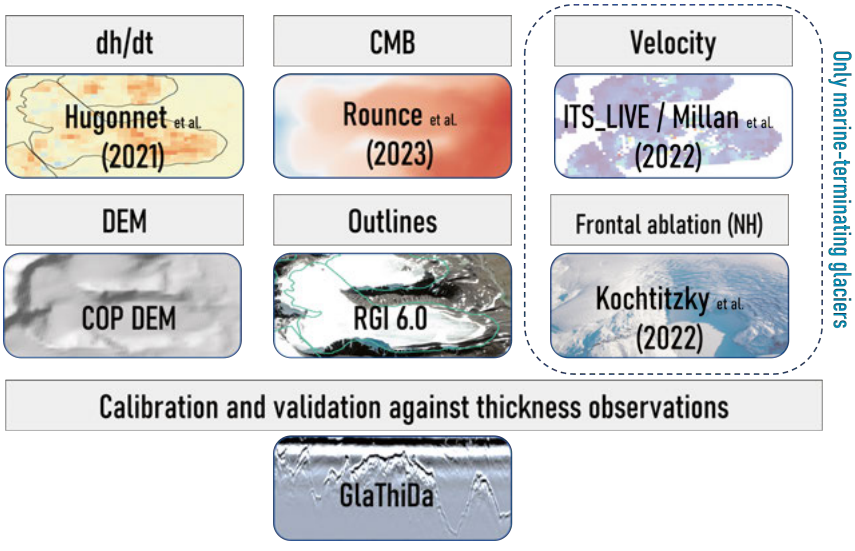

Figure 4.3. Input data sets used in Paper IV. For the other papers, equivalent datasets though partly from different sources were used.

century. It was used in Paper II, III, and IV while Paper I used manually delineated outlines. RGI version 6.0 (v6.0) was released by the RGI Consortium in July 2017 (RGI Consortium, 2017). A newer version 7.0 is available since 2023 but was not used in this thesis due to incompatibility of other input data products with the new data set. RGI v6.0 contains 215,547 individual glacier polygons and reports a total glacierized area of 705,738.8 km^2. The inventory is organized into 19 first-order regions originally defined by Radić and Hock (2010) and 91 second-order regions (Fig. 1.1).

The dataset is distributed as ESRI ArcGIS shapefiles, accompanied by regional attribute tables and a hypsometry file for each region. Each glacier polygon is associated with a 14-character identifier and a standard set of attributes that include source date fields, centroid coordinates, area, minimum and maximum elevation, median elevation and typology flags. Glaciers with a smaller area than 0.01 km^2 are not included (Pfeffer et al., 2014). The RGI was compiled from a mixture of new digitizations and numerous regional and legacy inventories. In Scandinavia, for instance, the outlines were retrieved from a previous mapping effort by Andreassen et al. (2012). For Svalbard, the mapping was originally carried out by Nuth et al. (2013).

While ideally representing glacier extents in the year 2000, data availability challenges and limited resources to carry out the laborious mapping have resulted in some deviations from this target. In v6.0, 49% of glacier outlines are from 2000 $\pm$ 2 years, and 43% were acquired within 2000 $\pm$ 2-10 years. The remaining 8% of outlines are more than 10 years older or younger than the target year 2000. The RGI is affected by errors in mapping the outlines accurately

(Pfeffer et al., 2014). A predominant error source is the distinction between seasonal snow and glacier. In addition, geolocation errors of the outlines and mapping of debris-covered glaciers are known issues.

Despite its limitations, the RGI is a cornerstone of many large-scale glacier studies. It has been used extensively as a starting point for future modeling (e.g. Rounce et al., 2023; Zekollari et al., 2025; Schuster et al., 2025), to guide the generation of key observational products (e.g. Hugonnet et al., 2021; Millan et al., 2022; Gardner et al., 2022) and to determine the global glacier volume (e.g. Grinsted, 2013; Farinotti et al., 2019a; Millan et al., 2022).

4.2.2 Surface elevation

Surface digital elevation models (DEMs) hold the key information for inferring the bed shape. As described in Sec. 3.2, features visible on the glacier surface represent a much larger feature on the glacier bed, underscoring the importance of accurate and noise-free DEMs. In Paper I, a DEM based on Pléiades imagery and specifically made for the glacier Kronebreen was used (Deschamps-Berger et al., 2019). Pléiades imagery, acquired by the twin Pléiades-1A and -1B satellites, offers very high spatial resolution (0.5 m to 2 m) and the capability to acquire along-track stereo pairs suitable for DEM generation, with vertical accuracies of a few meters (Deschamps-Berger et al., 2019). In Paper II, national DEMs of Norway and Sweden were applied (Kartverket, 2013; Lantmäteriet, 2022). For Paper III, a DEM based on aerial imagery specifically made for Svalbard was used (NPI, 2014) and finally, Paper IV saw the application of the global Copernicus DEM (COP DEM; ESA and Airbus, 2019). This DEM is based on the TanDEM-X DEM, created from bistatic X-band interferometric radar measurements by the TerraSAR-X and TanDEM-X satellites between 2010 and 2015 at 0.4 arcsecond posting. The COP DEM is a harmonized and edited version of the TanDEM-X DEM with void filling and correction of radar shadowing effects (ESA and Airbus, 2019). Other DEMs with large-scale or global coverage could have been applied in Paper IV instead. These include the Shuttle Radar Topography Mission DEM (Farr and Kobrick, 2000) and the Advanced Spaceborne Thermal Emission and Reflection Radiometer Global DEM (Abrams et al., 2020). However, based on evaluations done in the OGGM framework (Maussion et al., 2019) the COP DEM was chosen.

DEMs exhibit limitations when applied in mountainous or glacierized regions (Frey and Paul, 2012; Chen et al., 2022). Steep slopes, cast shadows, and radar layover effects in synthetic aperture radar-based DEMs often result in elevation errors or voids, particularly on glacier tongues, steep valley walls, and shaded terrain. Optical DEMs can suffer from poor stereoscopic matching in snow-covered or low-texture regions, leading to unrealistic surface artifacts. Consequently, vertical accuracies typically degrade in rugged mountain regions.

4.2.3 Mass balance and surface height change

In recent years, a number of global and regional data products have emerged that, when combined, permit a near-full closure of a glacier's mass budget. The three key components for that are dh/dt, climatic mass balance and frontal ablation. Mass budget closure implies that

$$\int_{\Omega} \dot{b} - \int_{\Omega} \frac{dh}{dt} = a, \tag{4.4}$$

where Ω is the glacier domain and a is frontal ablation, i.e. the mass loss through calving and melt at the ice-ocean interface. While Paper I relied on local data sets not described here, the subsequent papers all used the global dh/dt dataset by Hugonnet et al. (2021). Paper III used the climatic mass balance produced by van Pelt et al. (2019) with Paper II and IV relying on the global product from Rounce et al. (2023). Frontal ablation a can either be derived as the residual of Eq. (4.4) or it can be taken from observations. The latter was done in Paper IV using the products by Kochtitzky et al. (2022) and Fürst et al. (2024). Due to the absence of frontal ablation estimates for peripheral Antarctic glaciers, a was a calibration factor for those glaciers in Paper IV.

Hugonnet et al. (2021) produced a global dh/dt product at 100 m spatial resolution. The product is constructed by stacking and cross-registering satellite DEMs and altimetry datasets and applying corrections for biases and seasonal sampling, thereby yielding a geodetic estimate of glacier thinning or thickening. Combined with an estimate on the density of the elevation change, their output gives the observed mass change per grid cell. The density used throughout this thesis to convert elevation to mass change was 850 kg m^{-3} following Huss (2013). The temporal coverage of the dh/dt dataset spans the 2000–2019 period with elevation change grids available in 5-year bins. However, these may show considerable noise, implying that the most reliable signal is obtained from the full 20-year average.

Rounce et al. (2023) provide a globally consistent climatic mass balance dataset, derived from the mass balance model PyGEM calibrated to the dh/dt observations from Hugonnet et al. (2021) and validated against point mass balance observations from WGMS (2022). Their product gives, for each glacier, an elevation-dependent climatic mass balance gradient per year. Rounce et al. (2023) further supply future projections of glacier mass balance under different climate scenarios, but for the inversion context of this thesis the hindcast period 2000-2019 was used for which the product may be regarded as a reanalysis product. The average of these years was calculated to make climatic mass balance and dh/dt directly comparable.

The climatic mass balance for Paper III was taken from van Pelt et al. (2019). This dataset is generated at 1 km horizontal and 3-hourly temporal resolution. Their modeling framework is a coupled energy-balance and multi-layer sub-

surface hydrological/thermal model, forced by downscaled regional climate model output. Observational data (stake mass balance, automatic weather stations, snow core density profiles, temperature records) are used extensively for calibration and validation. The period 2010-2019 was used in Paper III.

Kochtitzky et al. (2022) compiled, for all Northern Hemisphere marine-terminating glaciers, estimates of frontal ablation, defined as the sum of ice discharge through flux gates and mass change associated with terminus retreat or advance. Their product includes decadal means (2000–2010, 2010–2020) of discharge magnitude, terminus mass change, and total frontal ablation in Gt yr^{-1}. The estimates draw on available velocity observations, terminus mapping from satellite imagery, and assumptions for thickness at flux gates and depth-averaged velocity. They note that many glaciers contributing most of the frontal ablation have at least one thickness observation along flux gates, although there also are marine terminus glaciers that still lack direct thickness data — here they fill in with bias-corrected model data from Millan et al. (2022). The annual mean frontal ablation over the full period 2000-2020 was used. The product by Fürst et al. (2024) was used for Patagonian glaciers in Paper IV. It is a combination of observations and model output representing the year 2000.

4.2.4 Ice flow velocities

Observed ice flow velocities were used to constrain the basal friction coefficient. This was done in Paper I, III and IV. In Paper II, no spatially distributed inversion for this parameter was performed. Instead, a regionally uniform value was calibrated against thickness observations. The observational ice velocity products used were ITS_LIVE (Inter-mission Time Series of Land Ice Velocity and Elevation; Gardner et al., 2022) and a product by Millan et al. (2022).

The ITS_LIVE dataset provides near-global, multi-decadal ice velocity fields derived from optical feature tracking applied to Landsat 4–8 imagery. It offers annual to sub-annual velocity composites at 120 m spatial resolution from 1985 to the present, with estimated uncertainties typically below 5 m yr^{-1} for slow-flowing ice and larger in regions of steep terrain or data scarcity (Gardner et al., 2022). The dataset by Millan et al. (2022) combines interferometric synthetic aperture radar and optical feature tracking from multiple sensors, including Sentinel-1, Sentinel-2, and Landsat-8, to produce a global map of surface ice flow at 100 m resolution for nearly all glaciers outside the ice sheets. The acquisition period for this product was 2017/18. The dataset provides full spatial coverage, including high-latitude and polar regions where optical data are often limited. In Paper I, a validation of the Millan et al. (2022) dataset with stake velocities showed very good performance on Kronebreen. However, this is not necessarily representative of other glaciers or regions. For slow-flowing

glaciers, for instance, this product often depicts highly noisy velocity fields. Indeed, both products share limitations — particularly in areas with persistent cloud cover, low surface contrast, strong seasonal variability or slow flow (Gardner et al., 2022; Millan et al., 2022). Moreover, errors may arise from temporal averaging and differing acquisition dates across sensors.

4.2.5 Thickness observations

Direct observations of the glacier bed and ice thickness are key in an inversion context to calibrate and validate the models. Such observations are obtained through a variety of direct and geophysical methods (Welty et al., 2020). The most direct approach is borehole drilling, which yields point measurements of ice thickness at a specific location, but is costly, logistically demanding, and spatially limited (Pohjola, 1993). More commonly, GPR is used, where electromagnetic waves propagate through the ice and reflect at the ice–bedrock interface (Bogorodsky et al., 1985; Flowers and Clarke, 1999). This approach can produce denser transects or grids of thickness data, often coupled with GPS for georeferencing. Seismic methods have also been applied in some settings, relying on acoustic wave propagation through ice and bedrock (Susstrunk, 1951). Despite several decades of efforts to measure ice thickness, the data record is still extremely sparse in relation to the global glacier-covered area. To facilitate integration of these observations with large-scale studies, the Glacier Thickness Database (GlaThiDa) was established (Gärtner-Roer et al., 2014; Welty et al., 2020) as a compilation of publicly available observations from numerous studies. The first published version (Gärtner-Roer et al., 2014) compiled data from roughly 1,100 glaciers, with some 750,000 point observations and glacier-wide estimates of mean and maximum thicknesses. In its more recent version (v3; Welty et al., 2020), the GlaThiDa contains 3,854,279 thickness measurements across $\sim$3,000 glaciers globally. Approximately 14% of global glacier area is now within 1 km of at least one thickness observation on the same glacier. A new v4-beta is now available online and continuously accepting contributions. Despite this growth, many glaciers remain poorly sampled: in some regions (e.g. Asia, Russian Arctic, and the Andes) coverage is particularly sparse.

Data from the GlaThiDa was used in all papers of this thesis. However, using these observations in thickness or volume estimation entails several caveats. First, uncertainties in the original measurements (e.g. due to signal scattering, multiple bed reflections, dielectric velocity assumptions, geolocation issues) can be substantial and metadata is sometimes poorly documented. Second, sampling is biased toward accessible glacier tongues or transects, meaning headwall regions or steep zones are often underrepresented, which can distort thickness estimates if the observed data are not representative of the full bed morphology (Farinotti et al., 2021). Third, the timing of data acquisi-

tion is often mismatched with other input data sets, requiring corrections for time-dependent surface changes in case the observations are reported as ice thicknesses instead of bed elevations. Finally, reported mean and maximum glacier thicknesses need to be interpreted with care as the limited radar observations used to establish them may not actually be representative of the full ice distribution within a given glacier.

Lomonosovfonna
Svalbard

Photo: Thomas Frank

5. Summary of papers

This chapter presents the key results of this thesis, going from the initial method development and testing via regional studies to the final global application. Although all studies rely on the methodology presented in Sec. 4.1 there are important differences between them pertaining to study region, input data, ice flow model and output interpretation.

5.1 Testing the new thickness inversion method

The development of the inversion method described in Section 4.1, first test applications and sensitivity experiments were presented in Paper I. Specifically, the initial testing was performed on a synthetic ice cap, on the glacier Kronebreen in Svalbard, and on synthetic glaciers from the Ice Thickness Model Intercomparison Experiment phase I (ITMIX; Farinotti et al., 2017).

Under an idealized setup with exactly known boundary conditions and ice-flow physics, the method was found to converge to the true bed topography. Recovering the basal friction coefficient from synthetic "observed" velocities was shown to be both feasible and essential for accurate bed inversion under slippery basal conditions. A key finding for subsequent studies was that convergence requires many bed updates using the dh/dt misfit, while friction updates based on velocity misfits are needed only a few times during the inversion. Several sensitivity experiments were performed by perturbing the known boundary conditions to emulate real-world data imperfections. These experiments revealed that: (1) surface mass flux errors (i.e., dh/dt or $\dot{b}$) only mildly affect the estimated glacier volume; (2) the choice of θ strongly influences the inferred bed geometry, with larger θ values yielding smoother beds and stronger dependence on initial conditions, but allowing for better accommodation of surface elevation errors; and (3) errors in observed velocities and surface mass flux are more detrimental in joint inversions for bed and friction than in bed-only inversions, whereas errors in ice viscosity can be compensated through friction inversions.

The subsequent application to Kronebreen, chosen due to an abundance of available input data and thickness observations, using the ice-flow model PISM produced promising results with low bed elevation and surface velocity discrepancies across most of the glacier (Fig. 5.1a,b). However, one area exhibited large deviations, attributed to limitations of the SIA that caused misalignment between modeled and observed flow directions (Fig. 5.1c). A post-processing step was introduced to address this issue, after which the inverted

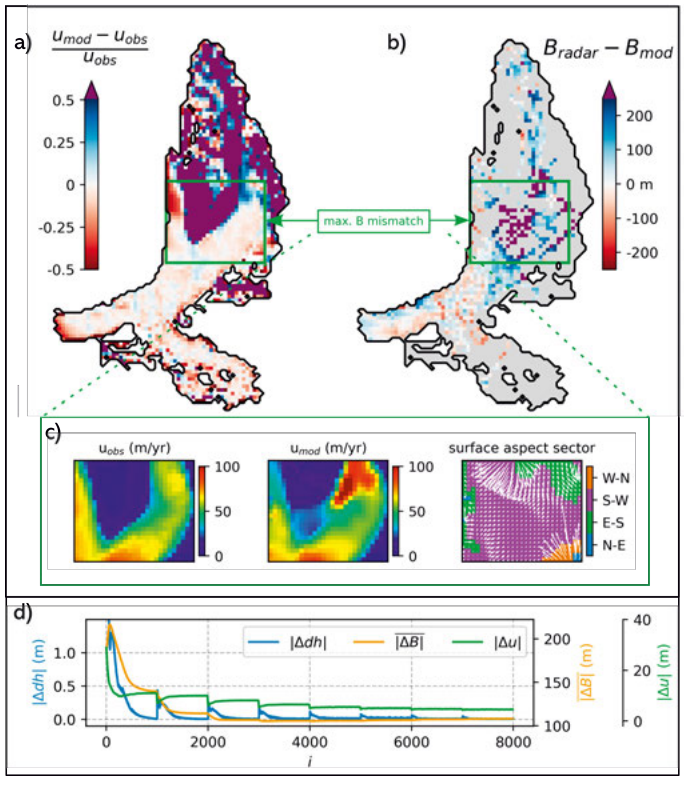

Figure 5.1. Output of Kronebreen inversion from Paper I. a) Spatially distributed velocity misfit; b) bed misfit at location of observed thicknesses; c) observed and modeled velocities in area with largest bed misfit, highlighting differences in flow directions related to the aspect of the surface slope; d) reduction of several misfit terms over the course of the iterations.

thicknesses showed smaller misfits to observations than results from previous studies.

Benchmarking the method against synthetic reference test cases from ITMIX demonstrated excellent performance, ranking it first or second among participating models across several metrics. Overall, the method proved computationally efficient and robust, achieving convergence to physically consistent bed solutions in all tested cases (e.g., Fig. 5.1d). As anticipated from its design, the post-inversion model state was found suitable for prognostic simulations without additional spin-up.

5.2 Refined regional ice volumes and bed topographies

Papers II and III both involved the application of the new inversion method on a regional scale. This required upscaling the approach to make it applicable to a large number of glaciers using the regional or global scale datasets described in Sec. 4.2. Critical to this task was to merge connected glaciers into glacier complexes in order to avoid artificial steps in bed topography between them. In addition, a method was developed to harmonize dh/dt and mass balance input data through the concept of the apparent mass balance (Farinotti et al., 2009), defined as $\tilde{b} = \dot{b} - \frac{dh}{dt}$, that allowed to fit a piece-wise linear function over elevation with the constraint $\int_\Omega \tilde{b} = 0$ for land-terminating glaciers where Ω is the glacier domain. Furthermore, both studies relied entirely (Paper II) or partly (Paper III) on the physics-informed deep-learning model IGM (Jouvet and Cordonnier, 2023) as a way to reduce computational costs while employing higher-order ice flow physics.

5.2.1 Scandinavia

The first regional-scale application of the inversion method was conducted in Scandinavia, hosting 3,417 land-terminating glaciers according to the RGI v6.0 (Andreassen et al., 2012; RGI Consortium, 2017). While Norway is home to the majority of those (n = 3,130 glaciers) and has several large ice caps, Sweden's glaciers are generally small mountain glaciers. Using only globally available data products — except for the DEMs — and the computationally efficient higher-order ice-flow model IGM (Jouvet and Cordonnier, 2023) this study represented an important test case toward the subsequent global application of the method.

Since no friction inversion was performed, region-wide uniform sliding and ice viscosity coefficients were tuned simultaneously by placing both parameters on a single continuous scale (effectively merging them into one) and calibrating them against observed ice thicknesses. The thickness observations were obtained from the GlaThiDa (Gärtner-Roer et al., 2014; Welty et al.,

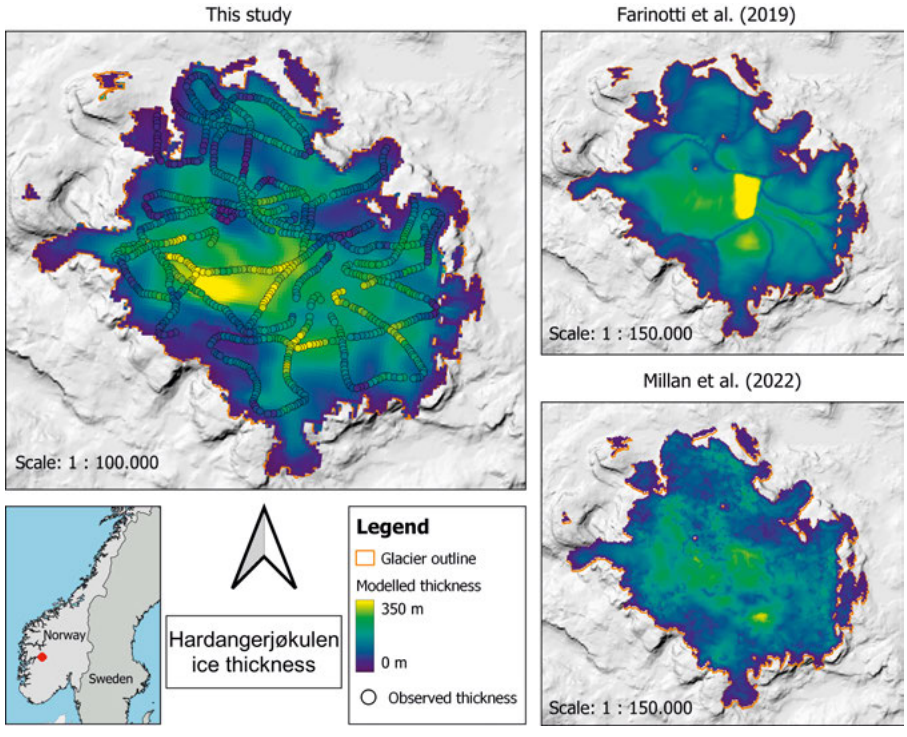

Figure 5.2. Modeled ice thickness for Hardangerjøkulen ice cap from this study as well as Farinotti et al. (2019a) and Millan et al. (2022). Overlain on the results of this study are observations of ice thickness from the Glacier Thickness Database (GlaThiDa Consortium, 2020)

.

2020) and complemented by a bed DEM for Storglaciären (Björnsson, 1981). Uncertainties in the computed volumes were estimated by evaluating the range of parameter combinations required to match the thickness observations across individual observed glacier complexes.

The resulting products comprise 100 m resolution ice thickness and bed elevation rasters for all glaciers in Scandinavia (Fig. 5.2). The total ice volume, representative of approximately the year 2010, was estimated at 321.1 km^3, with 302.7 km^3 located in Norway and 18.4 km^3 in Sweden, and an associated uncertainty of about 11%. The corresponding SLE from Scandinavian glaciers was calculated as 0.81 mm. Comparison with "known" ice volumes of well-observed glaciers showed excellent agreement, with all observed volumes falling within the modeled uncertainty ranges. The estimated regional ice volumes were larger than those from all but one previous study, though generally consistent within uncertainties. The largest significant deviations occurred relative to early global studies by Radić and Hock (2010), Marzeion et al. (2012), and Huss and Farinotti (2012). The study provided unprecedented detail in bed

topography, as demonstrated by evaluating model performance against bed observations using several different metrics. Bias and RMSE were lower, while both the correlation coefficient and the difference in bed roughness were improved, indicating more realistic and less overly smoothed beds compared to previous products (Farinotti et al., 2019a). Indeed, earlier global studies producing distributed bed elevation grids for the region (Farinotti et al., 2019a; Millan et al., 2022) were found to exhibit unrealistic features, such as artificial "walls" between flow units of ice caps or highly noisy bed structures (Fig. 5.2).

The openly available bed and thickness rasters constitute valuable datasets for future modeling studies in Scandinavia and for assessing the impacts of glacier retreat on the evolving landscape. To further improve model calibration in future work, additional bed observations from Swedish glaciers were identified as particularly valuable.

5.2.2 Svalbard

Another regional-scale application of the inversion method was carried out for Svalbard (excluding the island of Kvitøya), which hosts 1,544 glaciers covering a total area of 33,775 km^2 (Nuth et al., 2013; RGI Consortium, 2017). In contrast to Scandinavia, a large fraction of Svalbard's glacierized area (71%) consists of tidewater glaciers. Moreover, at least 103 glaciers are of surge type, 13 of which were actively surging during the study period (2015–2018) (Koch et al., 2023). Given the previously untested ability of IGM (Jouvet and Cordonnier, 2023) to simulate tidewater glaciers, and the challenges associated with inverting ice thickness for surging glaciers, three distinct inversion approaches were employed. One approach was practically identical to the one in Paper II and was applied to small land-terminating glaciers at 100 m spatial resolution (for the exact definition of the three glacier classes, refer to the manuscript). Another approach followed the new inversion method (Sec. 4.1) but employed the ice-flow model PISM (as in Paper I), targeting large and marine-terminating glaciers at 500 m resolution. Owing to the pronounced basal sliding of tidewater glaciers, this approach included a friction inversion (Eq. (4.3)). Finally, surging glaciers were modeled using a simpler perfect-plasticity method (Nye, 1952) at 500 m resolution because unavoidable mismatches in input data acquisition time would have lead to large errors using the iterative inversion method. This paper has two main authors that contributed equally - the author of this thesis who focused on the inversion using IGM and Ward van Pelt who led the PISM and perfect plasticity inversions.

The input data comprised both high-quality regional products (DEM from NPI (2014) and mass balance from van Pelt et al. (2019)) and globally available datasets described in Sec. 4.2. Calibration was achieved by tuning θ (Eq. (4.3)) and a mass balance correction factor M_{corr} in the PISM approach; by jointly calibrating a spatially constant friction parameter and ice viscosity in the IGM

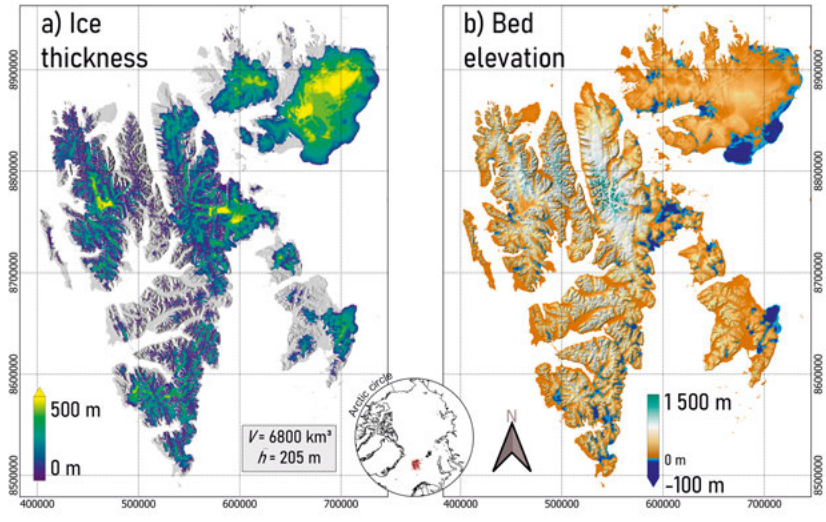

Figure 5.3. Ice thickness (a) and basal topography (b) for all glaciers in Svalbard (excluding Kvitøya).

approach (as in Paper II); and by adjusting the yield stress and slope threshold in the perfect-plasticity approach. In each case, the parameters were optimized to minimize the misfit between modeled and observed ice thicknesses. Volume uncertainties were estimated by evaluating the distribution of ice thickness biases for individual observed glaciers.

The primary output were ice thickness and bed maps for all Svalbardian glaciers (Fig. 5.3). The Svalbard-wide total ice volume, representative of the period 2010-2015, was found to be 6,800$\pm$238 km^3, corresponding to a SLE of 16.3$\pm$0.6 mm. The on average thickest glaciers were found in the Northeast while the Northwest hosts the thinnest ones. Despite a much larger number of land-terminating glaciers, the majority of ice is held in marine-terminating ones (80%). Only 4%, 24% and 45% of present-day ice volume is above the projected equilibrium line altitude (ELA) for 2060 (van Pelt et al., 2021) in Southern, Northwestern and Northeastern Svalbard, respectively, making glaciers highly vulnerable to future climatic changes. Because surface lowering associated with future mass loss will further move ice from higher to lower elevations, the actual ice volume remaining above the ELA after equilibration to the new climate is expected to be even smaller. Comparison with thickness observations showed strong statistical agreement, with RMSE values of 75.5 m for glaciers modeled using PISM and the perfect-plasticity approach, and 49.2 m for those modeled with IGM. The corresponding bias and correlation coefficient (R) were 0.2 m and 0.81 for the former, and 0.6 m and 0.78 for the latter. When compared to the only other available study that did not

fully assimilate the thickness observations (Millan et al., 2022), and for which a meaningful comparison was therefore possible, the new product was deemed superior given these statistical measures. Further comparison with the results of Millan et al. (2022) and Fürst et al. (2017) — the latter having fully assimilated bed observations — revealed notable differences. Whereas the spatial ice thickness distribution was found to be more similar to Fürst et al. (2017), the total volume closely matched that of Millan et al. (2022). Overall, the use of three distinct yet complementary inversion methods proved advantageous. The openly available bed maps represent a valuable resource for future glaciological and broader Earth system studies.

5.3 Global ice volume, bed topography and potential future lakes

In Paper IV, the inversion method previously applied to Scandinavia and Svalbard was extended to all glaciers on Earth, resulting in a globally complete dataset of glacier bed topography and ice thickness. Using the RGI v6.0 outlines (RGI Consortium, 2017) as the glacier mask and compiling a suite of global datasets of surface elevation, elevation change, ice velocity, and climatic mass balance (Sec. 4.2), IGM was used to infer spatially distributed ice thickness and bed elevation. The model calibration relied on more than 3.8 million ice thickness observations from the GlaThiDa (Gärtner-Roer et al., 2014; Welty et al., 2020) to constrain several model parameters regionally, using Bayesian methods (Nogueira, 2014). The results provide a consistent set of 100–400 m resolution maps of ice thickness, bed elevation, and the location and depth of overdeepenings that could host lakes in the future.

The total ice volume contained in glaciers globally was found to be $149.41 \pm 29.00 \times 10^3$ km^3, corresponding to a SLE of 316 ± 61 mm (Fig. 5.4). This estimate is considerably lower than older estimates (Dyurgerov and Meier, 2004; Radić and Hock, 2010; Marzeion et al., 2012; Huss and Farinotti, 2012; Radić and Hock, 2014), although broadly consistent with, but in between, other recent global studies by Farinotti et al. (2019a) and Millan et al. (2022). Despite similar overall volumes, significant regional differences to Farinotti et al. (2019a) and Millan et al. (2022) were found that could partly be explained by simpler methodological choices of the previous studies. Marine-terminating glaciers, though representing only about 2% of the global glacier count, were found to hold roughly 60% of the total ice volume, underscoring their importance for global sea-level projections (Fig. 5.4).

From the reconstructed bed topographies, overdeepenings capable of retaining water after a hypothetical complete deglaciation were identified using a hydrological sink-filling algorithm (Zhou et al., 2016). This analysis revealed 56,659 depressions capable of hosting potential future lakes, corresponding to a combined area of 40,647 km^2 and a total volume of 3,138 km^3 (Fig. 5.5). The

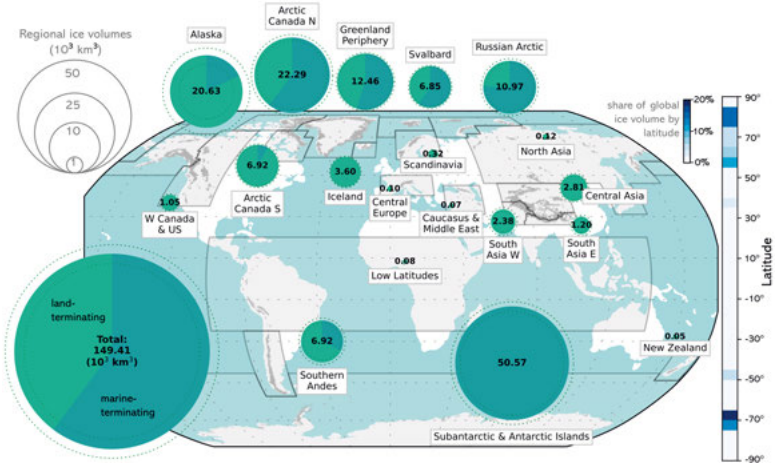

Figure 5.4. Global and regional glacier volumes (in 10^3 km^3) by RGI region. Light and dark green portions of pie charts reflect volume stored in land- and marine-terminating glaciers, respectively. Dashed circles show volume uncertainties. Blue bar on the right indicates glacier volume aggregated by latitude.

resulting water storage above sea level amounts to about 7 mm SLE, equivalent to roughly 2% of the total glacier SLE. The newly deglaciated terrain would feature approximately three times more lake area per land area than today's ice-free landscapes. The largest concentrations of potential future lakes were found beneath gently sloping glaciers, such as those in the Arctic, while steep mountain ranges such as the European Alps and Andes exhibited a far smaller density of overdeepenings (Fig. 5.5).

Comparison against available thickness observations demonstrated good agreement, with statistical performance similar to that achieved by previous studies, though an entirely independent, large-scale validation is not possible due to all studies using all available observations for calibration (Farinotti et al., 2019a; Millan et al., 2022). However, in contrast to the previous globally available bed maps, the results showed overall realistic bed geometries, avoiding unphysical artifacts such as artificial discontinuities between adjacent glaciers or highly noisy bed shapes. These advancements were directly linked to the methodology behind the different studies, with the key advantage of Paper IV being the application of higher-order ice-flow physics on distributed grids. Nevertheless, uncertainties linked to the large-scale approach of the study remain at the local scale (Sec. 3.3).

Beyond providing updated estimates of global ice volume and potential future lakes, the new global bed topography dataset called *Topography of a Deglaciated Earth v1.0* (TOPO-DE v1.0) can serve as a baseline for future modeling of glacier dynamics, meltwater routing, and landscape evolution. The maps of potential future lakes highlight regions where new water bod-

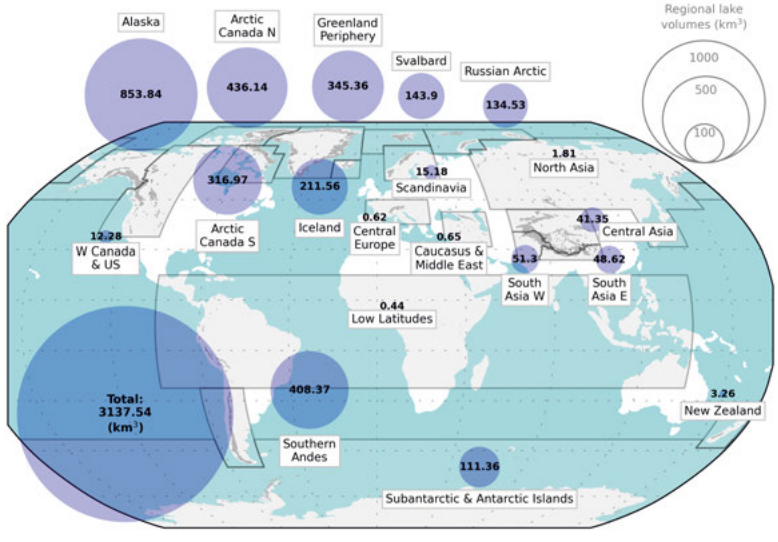

Figure 5.5. Global and regional potential lake volume in currently glacierized terrain.

ies are likely to emerge as glaciers retreat, offering valuable information for hydro- and ecological studies as well as for assessing potential hazards, such as glacier lake outburst floods. Altogether, the results offer a comprehensive view of the landscapes beneath Earth's glaciers. Methodologically, the study was the first to apply a higher-order model on distributed grids to all glaciers globally, progressing from earlier SIA and flowline based approaches.

Kennicott Glacier
Alaska

Photo: Thomas Frank

6. Outlook

Motivated by the so-far insufficient knowledge on the spatial distribution of glacier ice on Earth, this thesis provides new constraints on the ice thickness, bed topography and glacier volume on regional and global scales. A novel thickness inversion method was developed that goes beyond previous approaches that are based on strong simplifications of the ice-flow physics. After initial testing and bench-marking, this method found applications in Scandinavia, Svalbard and finally on all glaciers globally, redefining the view on the subglacial landscapes that may soon emerge from beneath the ice. The key outcomes of this thesis may be divided into methodological advancements and new data of direct practical relevance.

Methodologically, the central outcome of this work is the development of a glacier thickness inversion method that is 1) computationally efficient, and easy to implement, 2) model agnostic and compatible with complex ice-flow physics, 3) reliably stable and 4) allows for joint inversions with basal friction. Although applied in a thickness inversion framework here, this method could also be used to infer other hard-to-observe glacier characteristics, such as ice viscosity, provided that a heuristic gradient function can be established similar to Eq. (4.1). While it remains to be tested, it seems likely that a further development of the method could also infer more than the two parameters (thickness and friction) simultaneously. This would be contingent on the number of corresponding target observations increasing as well, and on the signal from different processes being clearly disentangible. For instance, it would seem relatively straight-forward to also infer a calving parameter that controls the position of the glacier front, using observations of the latter. Meanwhile, inferring distributed ice viscosity and sliding simultaneously in addition to bed topography may be more difficult, given that both reflect predominantly on ice flow velocities, and that it would be unclear how to separate the influence of varying the two parameters.

The inverse method has strong potential for further applications in local and regional studies. Furthermore, a repeat application on a global scale, once better input data become available, seems promising to update the global bed product TOPO-DE and reduce errors linked to input data uncertainties. Similarly, the method could be applied on an ice-sheet scale to provide a new bed product there. Meanwhile, the method itself could also see further improvements to enhance its wider applicability. This could include a currently lacking ability to locally, rather than globally, assimilate thickness observations. Also, 'mass leakages' where a non-zero ice thickness is produced outside the

defined glacier domain have proven to be a challenge. To resolve both of these aspects ideally requires the inclusion of long-range model sensitivities in the inversion, i.e. to move away from bed updates that are applied as a function of the local misfit alone. Mathematically speaking, this would require to replace the identity matrix as the model Jacobian with a matrix with non-zero values at the off-diagonal entries. How to implement this without computing the full Jacobian or the adjoint model which would increase the complexity of the method considerably and take away its key strengths needs to be explored further. Furthermore, the method is currently not optimally equipped to take input data errors into account. In contrast to variational methods where different cost functions terms can be assigned different weights, or when using regularization methods that ensure that the data is not fit beyond its uncertainties, the regularization technique used here based on surface updates is less explicitly linked to input data uncertainty. Due to the large-scale perspective of this thesis work, with overall poorly quantified input data errors and a general lack of thickness observations, such issues were not found critical. However, in cases where accurate input data error estimates exist, or where many thickness observations are available, a variational method may be more suitable. Of particular interest in this regard are novel machine-learning methods that are fully differentiable by design and increasingly constrained by physics, avoiding both large computational costs and the complex derivation of adjoint models. Indeed, even beyond thickness inversions, such methods open the door to assimilate an unprecedented amount of data that is already available, but currently disregarded by all large-scale models. Apart from so-far neglected quantities such as observed snow-lines, a large potential lies in harvesting time-dependent data such as historic glacier extents or past ice flow velocities which, in principle, can be obtained for the entire satellite era.

Beyond inversions, another methodological advance of this thesis lies in the application of a distributed higher-order ice flow model on a global scale. This is the first application of such kind, going beyond previous SIA-based flowline models that to-date form the standard in large-scale glacier models. While arguments can be made in favor of simpler models, in particular regarding the overparameterization of glacier models, it is also clear that many glaciers are not well-represented by such approaches. It thus appears likely that future studies will increasingly explore distributed models with more complete ice flow physics, the feasibility of which was demonstrated in this thesis. At the base of this advancement lie novel developments in computer science which have brought forward highly efficient ice flow models, such as IGM. These are enabled not only by machine-learning techniques, but also by massively parallelized code running on Graphic Processing Units. With more and more such tools emerging, not the least in the field of physics informed deep learning, a key limitation of ice-flow modeling studies on glaciers and ice sheets alike, namely the large computational resources required, is increasingly overcome.

Apart from the described technical advancements, this thesis provided new data that is of high relevance not only for direct climate change mitigation and adaptation, but also for follow-on studies that can profit from the bed topography datasets produced here. The new numbers on present-day glacier volume and SLE held in glaciers in Scandinavia, Svalbard and globally are of direct relevance for coastal adaptation in view of large-scale glacier mass loss. Although the global ice volume estimated in this thesis is very similar to previous recent estimates, the discrepancies found on a regional level are an important outcome that highlight the uncertainty in all estimates which so-far is not adequately propagated into future projections. To reduce this uncertainty, this thesis identified the collection of more thickness observations as key, alongside further methodological advances described above allowing to fully assimilate the wealth of observational data available. In addition, the constraint on the water volume potentially stored in lakes that form as glaciers retreat is an important outcome of this work. Although small compared to the total volume of glacier ice globally, this quantity was so-far unknown, limiting our understanding of hydrological feedbacks that emerge as glaciers retreat. Indeed, explicitly modeling the location and depth of these potential future lakes is of high relevance locally where such lakes could either pose a threat (e.g. due to them causing catastrophic floods) or offer opportunities (e.g. in the context of hydropower production or recreation). Nonetheless, these results should also be interpreted with care and under due consideration of the limitations of this large-scale study at local scales. Future work could seek to improve linking input data and model errors in different regions to the projected lakes, a task outside the scope of this work. Furthermore, more explicitly taking into account how future geomorphic changes of the lakes, e.g. due to erosion, influence their shape and volume could be explored further.

The bed topography datasets provided by this thesis also offer many new research possibilities that have barely been explored in this thesis. The possibility to identify geological features in the new bed maps has been demonstrated for one specific area in Paper IV, but could be attempted on a much wider scale. Similarly, the morphology of the glacier beds revealed, as well as that of the potential future lakes, carries important information to study future species colonization or limnology. Linking projected glacier changes to hydrological models by taking into account bed shape and future lakes also offers exciting research avenues that are of high relevance for quantifying the impact of glacier mass loss on the broader hydrological cycle. Finally, and above all, the glacier beds can form an input to prognostic ice dynamics studies, thus helping to produce better projections of future glacier change. Knowing that the inversion method developed here provides fully-initialized glacier states, a follow-on study could leverage this to project glacier evolution directly following a thickness inversion.


Kennicott Glacier
Alaska
Photo: Thomas Frank

7. Sammanfattning på svenska

Glaciärisarna smälter av och minskar i volym över hela världen. Detta gäller inte minst alla de dalglaciärer och isfält som finns i kalla bergsområden, men ligger utanför de stora inlandsisarna på Anatrktis och Grönland. Dessa är denna avhandlingens fokus, och kallas för bara ”glaciärer” här. För att förbättra prognoserna för glaciärförändringar och bedöma därmed sammanhängande effekter på jordsystemet krävs noggrann kunskap om bottentopografin under isen. Direkta observationer av glaciärbotten finns dock endast för en liten del av de över ca. 200,000 glaciärerna globalt. Därför behövs dator-baserade beräkningsmetoder för att härleda bottenegenskaper från den av naturliga skäl mer tillgängliga ytdatan. Denna avhandling presenterar en metod för inversion av glaciärbotten och istjocklek samt dess tillämpningar för att ta fram isvolymer från glaciärer på regional och global skala.

Metoden har utformats för att vara beräkningsmässigt effektiv, robust och kompatibel med komplex isflödesfysik på rutnät. Tester på syntetiska och verkliga glaciärer visade att denna metod presterar väl jämfört mot andra metoder. Den första regionala tillämpningen resulterade i detaljerade botten topografier för Skandinavien, och en beräknad total glaciärvolym på 0.32×10^3 km^3, vilket motsvarar 0.8 mm global genomsnittlig havsnivåhöjning ifall all is skulle smälta i Skandinavien. I en senare tillämpning på alla glaciärer i Svalbard – där glaciärdynamiken är mer komplex – uppskattades volymen till 6.80×10^3km^3 (motsvarande 16.3 mm havsnivåhöjning) och det uppnåddes bättre överensstämmelse med observationer jämfört med tidigare studier. Slutligen gav en global tillämpning en total glaciärvolym på 149.41×10^3 km^3 (motsvarande 316.1 mm havsnivåhöjning). Medan den globala totalsumman stämmer överens med tidigare uppskattningar, identifierades betydande regionala skillnader. Utöver isvolymen producerade den globala studien fysiskt realistiska botten topografier och kartlade >50,000 potentiella framtida sjöar i terräng som för närvarande är täckt av glaciärer, med en total volym på 3,138 km^3 (2% av den globala glaciärvolymen) och en yta på >40,000 km^2.

Metodologiskt sett innebär denna avhandling ett framsteg inom storskalig inversion av glaciärtjocklek och presenterar den första globala tillämpningen av högre ordningens isflödesfysik på rutnät, vilket möjliggörs av digital djupinlärning och parallelliserad kod optimerad för grafikkort. De regionala och globala uppskattningarna av isvolymen är viktig data för anpassnings- och begränsningsstrategier relaterade till glaciärernas massförlust och havsnivåhöjningen, medan de framräknade bottenkartorna stödjer framtida forskning inom geovetenskaperna samt möjliggör förbättrade prognoser för glaciärförändringar.

Photo: Maurice van Tiggelen

8. Acknowledgments

Whoever has actually looked into the thesis and not just skipped to this section will have noticed the pictures between chapters. They were all taken while on field work in different icy places around the world, showing just how lucky I was with this PhD. This brings me to my first acknowledgment: thanks, Swedish tax payers, for funding this science! But really, it is the people that have given me this opportunity and the people that have shared this journey with me that deserve the biggest thanks.

My first big thanks go to my main supervisor **Ward**. Thank you for trusting me with this project, for being supportive from start to finish, for opening many opportunities, for weekly discussions, for sending me to conferences and field work around the world and for always making me feel valued and equal. I was your first PhD student and I can say you mastered this challenge phenomenally. I also want to thank my co-supervisors: thanks, **Regine**, for your inspiring enthusiasm for glaciers, but even more, for the very insightful discussions we had. Your feedback is always frank and never misses any weak spot, something I very much appreciate and that has certainly pushed me further. Thank you, **Rickard**, for introducing me to various aspects of field work and GPR. Your diligence and eye for detail are as admirable as are your determination and endurance in the field. Thanks also, **Ian**, for good times in Abisko.

But it wasn't only my supervisors that I learned a lot from in these past years. Many thanks also to the other members of the Glaciology group! **Veijo**, thanks for sharing a lot of valuable experiences, not the least in a fieldwork context, but also for your great social spirit. **Christian**, for fun stories about Canada and for letting me use your teaching resources in quite a few courses which I find are very well made. **Moon**, for joining me as the one other PhD student in the ICE group. Thank you, **Jie** and **Shivang** for broadening my horizon on remote sensing. And **Katrin** and **Johan**, I'm really glad you joined us and I look forward to working with you in the next years. The same goes for you, **Alice**, I'm very happy to see such a competent person taking over after me as the "thickness inversion PhD student". Thanks also to the staff at the Swedish Polar Research Secretariat for the training and support for the upcoming Antarctic field work.

Already the last months I have started to reflect on the fact that the PhD journey would soon end for many of us that started their PhD around the same time. And my conclusion hasn't changed: I am convinced that when we look back at this chapter in the future we will remember that it surely wasn't always easy, but also, *what an amazing time we had with this group of people*. So

where to start? Of course with the loyal members of the Geo football team! Thank you, **Kevin**, not only for your countless attempts at lobbing the ball to your team members, but also for your overall genuine happiness and generosity that you share in so many contexts. You are a key reason for why our community at Geo in the last 5 years was special. Thanks to the fastest man on the planet, intercepting my passes countless times, the person I could never play in a team with until he luckily joined Gupta, **Rich**. Your jokes (and imitations) really made my days! Thanks to you, **Ferran**, for showing up in Arctic gear for football when the temperatures dropped below 10°C, a mirror of your warm spirit that has been a true enrichment to the social life of this department. And how could I mention Ferran without mentioning **Ana**, although "loyal members of the Geo football team" certainly isn't a category you belong to? No worries, I forgive you for not fulfilling your thesis promise (until now) for the nice person you are otherwise ;) Thanks also to the one person who made the Geo goals look big in comparison to body size until you stood in front of her knowing that she wouldn't hesitate to defend with all she got (including hands), **Iana**. Speaking of hands, some team members should be handed a copy of the football rules instead of this thesis, right, **Koffi**? But no worries, you aren't the only one and be assured that your smiles and happiness would be much missed if you hadn't joined us. Many thanks also to the other loyal members of the football team that made Wednesday lunch breaks a true highlight for me: **Leo**, for attempting shots from any angle, and for sharing statistics teaching with me off the pitch; **Calum**, for sacrificing your toe and being a comrade from SU times; **Alok**, for whacking the ball into the bushes numerous times, and then swearing at yourself for not having converted this clear chance with an expected goals value of 0.001; **Aditya**, for being clinical in front of the goal; **Sebba**, for being the senior person with most appearances; **Murat**, for continuous commitment since several years; **Andra**, past captain of the team, for maintaining and passing on the legacy of the football matches; **Greta** and **Moa**, for increasing the ratio of females on the pitch; **Tora**, for representing the admin corridor. Last but not least, there is no way I could forget star commentator, VAR and feared critic **Meriem**. Thanks for keeping an eye on us while we play, and sharing your feedback afterwards in your happy and genuine way. Overall, thanks to everyone that made the football matches so much fun, even those I didn't mention here.

But beyond football, there were many other pub visits, board game nights, skiing trips or work breaks where I was lucky to spend time with really nice people. **Laura**, it feels like you've been at Geo forever, although you actually started 1.5 years after me. But I'm not the only one who thinks that you've been around (on this earth) for much longer than you actually have, right? ;) Thanks for being a very warm-hearted and generous person! And never one *Gilmore girl* by herself, so thanks also to you, **Makoto**, not the least for the very nice time in Japan. And **Nicola**, for your many happy laughs, although you of course would vigorously deny that you are a Gilmore girl. I look for-

ward to more cozy board game nights, also with **Max** and **Johan**. **Sara C.**, thanks for your passion for Svalbard. Most likely a wetland will eventually form where there are glaciers now, allowing you to stay in this beautiful remote luxury cabin that I didn't get to go to in the end. **Christoffer**, for a long time I honestly couldn't imagine Geo without you, and still I sometimes seem to hear your laugh somewhere in the corridors. Thanks for the many social events we shared! Likewise, thanks **Elena, Lucia, Hector, Faranak** and **Mehdad** for the numerous occasions where we got to spend time with each other. **Michael**, thank you for being the only other person understanding my cravings for pretzels and Weisswurst, although you without any doubt are a better Bavarian than me. **Emma**, you showed me another perspective, namely of what it is like to be a foreigner in Germany, sometimes an amusing and sometimes a shocking tale. **Zibi**, thanks for some really enjoyable chats and of course the great skiing! And of course, thanks to my office mates **Ting, Agnes, Elisa** and **Shije**. We may not be the most talkative office but I very much enjoy being with you.

One thing I actually learned a lot more about during my PhD than I would have initially suspected is meteorology. This is no doubt due to **Anna, Antonio, Cecilia, Erik N., Erik S. Erik Sch., Gabriele, John, Jacopo, Lichuan, Monica, Minchao, Melinda, Rohan, Sonja, Svitlana** and **Venu**. Thanks a lot! And then my horizon was genuinely broadened by the hydrologists **Benjamin, Claudia, Ekaterina, Fritjof, Giuliano, Jeanne, Johanna, Mamata, Marie, Omar, Riccardo, Roger, Sara L., Surabhi, Thomas G.**, thank you! Many thanks also to **Anjali, Fatima, Gabriella, Iman, Mariia, Maria D., Malin E., Nabil, Nicholas, Sofie, Shakti, Thomas S., Tomas, Veronica, Yunus** for the time spent together.

Slutligen, ett otroligt stort tack till **Hanna** och **Jonatan**! Ni var inte med på Geo, men ändå har ni en jättestor del i den här avhandlingen. Det är helt sjukt att tänka på allt vi har upplevt tillsammans de senaste åren, de otroligt många fina stunder vi tillbringade på kvällar, helger och semester. Det betyder jättemycket för mig att ha er som vänner! Und alles das gilt natürlich auch für dich, **Ramona**. Wo soll ich anfangen, wo soll ich aufhören um die letzten 5 Jahre zu beschreiben? Das Zitat "Vi är de goaste vänner" aus "Utvandrarna" comes to mind, und ich finde, so soll es bleiben!

And as I'm now submitting this thesis, the first snow flakes of the winter are falling outside the window. What a cheesy end to this journey...

Bibliography

Abdel-Fattah, D., Danielson, M., Ekenberg, L., Hock, R., and Trainor, S.: Application of a structured decision-making process in cryospheric hazard planning: Case study of Bering Glacier surges on local state planning in Alaska, Journal of Multi-Criteria Decision Analysis, 31, e1825, https://doi.org/10.1002/mcda.1825, 2024.

Abrams, M., Crippen, R., and Fujisada, H.: ASTER Global Digital Elevation Model (GDEM) and ASTER Global Water Body Dataset (ASTWBD), Remote Sensing, 12, 1156, https://doi.org/10.3390/rs12071156, 2020.

Adhikari, S. and Marshall, S. J.: Influence of high-order mechanics on simulation of glacier response to climate change: insights from Haig Glacier, Canadian Rocky Mountains, The Cryosphere, 7, 1527–1541, https://doi.org/10.5194/tc-7-1527-2013, 2013.

Andreassen, L. M., Winsvold (eds), S., Paul, F., and Hausberg, J.: Inventory of Norwegian Glaciers, no. 28-2012 in NVE Rapport, Norwegian Water Resources and Energy Directorate, Oslo, Norway, 2012.

Andreassen, L. M., Elvehøy, H., Kjøllmoen, B., and Belart, J. M. C.: Glacier change in Norway since the 1960s – an overview of mass balance, area, length and surface elevation changes, Journal of Glaciology, 66, 313–328, https://doi.org/10.1017/jog.2020.10, 2020.

Aschwanden, A. and Brinkerhoff, D. J.: Calibrated Mass Loss Predictions for the Greenland Ice Sheet, Geophysical Research Letters, 49, e2022GL099 058, https://doi.org/10.1029/2022GL099058, 2022.

Bahr, D. B., Meier, M. F., and Peckham, S. D.: The physical basis of glacier volume-area scaling, Journal of Geophysical Research: Solid Earth, 102, 20 355–20 362, https://doi.org/10.1029/97JB01696, 1997.

Bahr, D. B., Pfeffer, W. T., and Kaser, G.: Glacier volume estimation as an ill-posed inversion, Journal of Glaciology, 60, 922–934, https://doi.org/10.3189/2014JoG14J062, 2014.

Behn, M. D., Goldsby, D. L., and Hirth, G.: The role of grain size evolution in the rheology of ice: implications for reconciling laboratory creep data and the Glen flow law, The Cryosphere, 15, 4589–4605, https://doi.org/10.5194/tc-15-4589-2021, 2021.

Bezanson, J., Edelman, A., Karpinski, S., and Shah, V. B.: Julia: A fresh approach to numerical computing, SIAM Review, 59, 65–98, https://doi.org/10.1137/141000671, 2017.

Bintanja, R. and van der Linden, E. C.: The changing seasonal climate in the Arctic, Scientific Reports, 3, 1556, https://doi.org/10.1038/srep01556, 2013.

Bishop, C. M. and Nasrabadi, N. M.: Pattern recognition and machine learning, vol. 4, Springer, URL `https://link.springer.com/9780387310732`, 2006.

Björnsson, H.: Radio-Echo Sounding Maps of Storglaciären, Isfallsglaciären and Rabots Glaciär, Northern Sweden, Geografiska Annaler: Series A, Physical Geography, 63, 225–231, https://doi.org/10.1080/04353676.1981.11880037, 1981.
Blatter, H.: Velocity and stress fields in grounded glaciers: a simple algorithm for including deviatoric stress gradients, Journal of Glaciology, 41, 333–344, https://doi.org/10.3189/S002214300001621X, 1995.
Bogorodsky, V. V., Bogorodskiĭ, V. V., Bentley, C. R., and Gudmandsen, P. E.: Radioglaciology, Springer Science & Business Media, 1985.
Bolibar, J., Rabatel, A., Gouttevin, I., Galiez, C., Condom, T., and Sauquet, E.: Deep learning applied to glacier evolution modelling, The Cryosphere, 14, 565–584, https://doi.org/10.5194/tc-14-565-2020, 2020.
Bolibar, J., Sapienza, F., Maussion, F., Lguensat, R., Wouters, B., and Pérez, F.: Universal differential equations for glacier ice flow modelling, Geoscientific Model Development, 16, 6671–6687, https://doi.org/10.5194/gmd-16-6671-2023, 2023.
Bosson, J. B., Huss, M., Cauvy-Fraunié, S., Clément, J. C., Costes, G., Fischer, M., Poulenard, J., and Arthaud, F.: Future emergence of new ecosystems caused by glacial retreat, Nature, 620, 562–569, https://doi.org/10.1038/s41586-023-06302-2, 2023.
Brinkerhoff, D., Aschwanden, A., and Fahnestock, M.: Constraining subglacial processes from surface velocity observations using surrogate-based Bayesian inference, Journal of Glaciology, 67, 385–403, https://doi.org/10.1017/jog.2020.112, 2021.
Brinkerhoff, D. J., Aschwanden, A., and Truffer, M.: Bayesian Inference of Subglacial Topography Using Mass Conservation, Frontiers in Earth Science, 4, 8, https://doi.org/10.3389/feart.2016.00008, 2016.
Budd, W. F., Jenssen, D., and Smith, I. N.: A Three-Dimensional Time-Dependent Model of the West Antarctic Ice Sheet, Annals of Glaciology, 5, 29–36, https://doi.org/10.3189/1984AoG5-1-29-36, 1984.
Bueler, E. and Brown, J.: Shallow shelf approximation as a "sliding law" in a thermomechanically coupled ice sheet model, Journal of Geophysical Research: Earth Surface, 114, https://doi.org/10.1029/2008JF001179, 2009.
Bueler, E. and van Pelt, W.: Mass-conserving subglacial hydrology in the Parallel Ice Sheet Model version 0.6, Geoscientific Model Development, 8, 1613–1635, https://doi.org/10.5194/gmd-8-1613-2015, 2015.
Chen, W., Yao, T., Zhang, G., Li, F., Zheng, G., Zhou, Y., and Xu, F.: Towards ice-thickness inversion: an evaluation of global digital elevation models (DEMs) in the glacierized Tibetan Plateau, The Cryosphere, 16, 197–218, https://doi.org/10.5194/tc-16-197-2022, 2022.
Cheng, G., Morlighem, M., and Francis, S.: Forward and Inverse Modeling of Ice Sheet Flow Using Physics-Informed Neural Networks: Application to Helheim Glacier, Greenland, Journal of Geophysical Research: Machine Learning and Computation, 1, e2024JH000 169, https://doi.org/10.1029/2024JH000169, 2024.
Cheng, G., Krishna, M., and Morlighem, M.: A Python library for solving ice sheet modeling problems using physics-informed neural networks, PINNICLE v1.0, Geoscientific Model Development, 18, 5311–5327, https://doi.org/10.5194/gmd-18-5311-2025, 2025.

Christ, A. J., Bierman, P. R., Schaefer, J. M., Dahl-Jensen, D., Steffensen, J. P., Corbett, L. B., Peteet, D. M., Thomas, E. K., Steig, E. J., Rittenour, T. M., Tison, J.-L., Blard, P.-H., Perdrial, N., Dethier, D. P., Lini, A., Hidy, A. J., Caffee, M. W., and Southon, J.: A multimillion-year-old record of Greenland vegetation and glacial history preserved in sediment beneath 1.4 km of ice at Camp Century, Proceedings of the National Academy of Sciences, 118, e2021442 118, https://doi.org/10.1073/pnas.2021442118, 2021.

Clarke, G. K. C., Berthier, E., Schoof, C. G., and Jarosch, A. H.: Neural Networks Applied to Estimating Subglacial Topography and Glacier Volume, Journal of Climate, 22, 2146–2160, https://doi.org/10.1175/2008JCLI2572.1, 2009.

Cogley, J. G., Arendt, A. A., Bauder, A., Braithwaite, R. J., Hock, R., Jansson, P., Kaser, G., Moller, M., Nicholson, L., and Rasmussen, L. A.: Glossary of glacier mass balance and related terms, 2010.

Cook, S., Gillet-Chaulet, F., and Fürst, J.: Robust reconstruction of glacier beds using transient 2D assimilation with Stokes, Journal of Glaciology, pp. 1–10, https://doi.org/10.1017/jog.2023.26, 2023a.

Cook, S. J., Jouvet, G., Millan, R., Rabatel, A., Zekollari, H., and Dussaillant, I.: Committed Ice Loss in the European Alps Until 2050 Using a Deep-Learning-Aided 3D Ice-Flow Model With Data Assimilation, Geophysical Research Letters, 50, e2023GL105 029, https://doi.org/10.1029/2023GL105029, 2023b.

Cordonnier, G., Jouvet, G., Peytavie, A., Braun, J., Cani, M.-P., Benes, B., Galin, E., Guérin, E., and Gain, J.: Forming Terrains by Glacial Erosion, ACM Trans. Graph., 42, 61:1–61:14, https://doi.org/10.1145/3592422, 2023.

Cornford, S. L., Martin, D. F., Lee, V., Payne, A. J., and Ng, E. G.: Adaptive mesh refinement versus subgrid friction interpolation in simulations of Antarctic ice dynamics, Annals of Glaciology, 57, 1–9, https://doi.org/10.1017/aog.2016.13, 2016.

Courant, R., Friedrichs, K., and Lewy, H.: Über die partiellen Differenzengleichungen der mathematischen Physik, Mathematische Annalen, 100, 32–74, https://doi.org/10.1007/BF01448839, 1928.

Deschamps-Berger, C., Nuth, C., Pelt, W. V., Berthier, E., Kohler, J., and Altena, B.: Closing the mass budget of a tidewater glacier: the example of Kronebreen, Svalbard, Journal of Glaciology, 65, 136–148, https://doi.org/10.1017/jog.2018.98, 2019.

Dyurgerov, M. B. and Meier, M. F.: Mass balance of mountain and subpolar glaciers: a new global assessment for 1961–1990, Arctic and Alpine Research, 29, 379–391, URL https://www.tandfonline.com/doi/abs/10.1080/00040851.1997.12003259, 1997.

Dyurgerov, M. B. and Meier, M. F.: Glaciers and the changing Earth System: A 2004 snapshot, p. 118, 2004.

Edwards, T. L., Nowicki, S., Marzeion, B., Hock, R., Goelzer, H., Seroussi, H., Jourdain, N. C., Slater, D. A., Turner, F. E., Smith, C. J., McKenna, C. M., Simon, E., Abe-Ouchi, A., Gregory, J. M., Larour, E., Lipscomb, W. H., Payne, A. J., Shepherd, A., Agosta, C., Alexander, P., Albrecht, T., Anderson, B., Asay-Davis, X., Aschwanden, A., Barthel, A., Bliss, A., Calov, R., Chambers, C., Champollion, N., Choi, Y., Cullather, R., Cuzzone, J., Dumas, C., Felikson, D., Fettweis, X.,

Fujita, K., Galton-Fenzi, B. K., Gladstone, R., Golledge, N. R., Greve, R., Hattermann, T., Hoffman, M. J., Humbert, A., Huss, M., Huybrechts, P., Immerzeel, W., Kleiner, T., Kraaijenbrink, P., Le Clec'h, S., Lee, V., Leguy, G. R., Little, C. M., Lowry, D. P., Malles, J.-H., Martin, D. F., Maussion, F., Morlighem, M., O'Neill, J. F., Nias, I., Pattyn, F., Pelle, T., Price, S. F., Quiquet, A., Radić, V., Reese, R., Rounce, D. R., Rückamp, M., Sakai, A., Shafer, C., Schlegel, N.-J., Shannon, S., Smith, R. S., Straneo, F., Sun, S., Tarasov, L., Trusel, L. D., Van Breedam, J., van de Wal, R., van den Broeke, M., Winkelmann, R., Zekollari, H., Zhao, C., Zhang, T., and Zwinger, T.: Projected land ice contributions to twenty-first-century sea level rise, Nature, 593, 74–82, https://doi.org/10.1038/s41586-021-03302-y, 2021.

Ekblom Johansson, F., Bakke, J., Støren, E. N., Gillespie, M. K., and Laumann, T.: Mapping of the Subglacial Topography of Folgefonna Ice Cap in Western Norway—Consequences for Ice Retreat Patterns and Hydrological Changes, Frontiers in Earth Science, 10, URL https://www.frontiersin.org/articles/10.3389/feart.2022.886361, 2022.

Elverhøi, A., Lonne, O., and Seland, R.: Glaciomarine sedimentation in a modern fjord environment, Spitsbergen, Polar Research, 1, 127–149, https://doi.org/10.3402/polar.v1i2.6978, 1983.

ESA and Airbus: Copernicus DEM – Global and European Digital Elevation Model (COP-DEM), https://doi.org/https://doi.org/10.5270/ESA-c5d3d65, 2019.

Farinotti, D., Huss, M., Bauder, A., Funk, M., and Truffer, M.: A method to estimate the ice volume and ice-thickness distribution of alpine glaciers, Journal of Glaciology, 55, 422–430, https://doi.org/10.3189/002214309788816759, 2009.

Farinotti, D., Brinkerhoff, D. J., Clarke, G. K. C., Fürst, J. J., Frey, H., Gantayat, P., Gillet-Chaulet, F., Girard, C., Huss, M., Leclercq, P. W., Linsbauer, A., Machguth, H., Martin, C., Maussion, F., Morlighem, M., Mosbeux, C., Pandit, A., Portmann, A., Rabatel, A., Ramsankaran, R., Reerink, T. J., Sanchez, O., Stentoft, P. A., Singh Kumari, S., van Pelt, W. J. J., Anderson, B., Benham, T., Binder, D., Dowdeswell, J. A., Fischer, A., Helfricht, K., Kutuzov, S., Lavrentiev, I., McNabb, R., Gudmundsson, G. H., Li, H., and Andreassen, L. M.: How accurate are estimates of glacier ice thickness? Results from ITMIX, the Ice Thickness Models Intercomparison eXperiment, The Cryosphere, 11, 949–970, https://doi.org/10.5194/tc-11-949-2017, 2017.

Farinotti, D., Huss, M., Fürst, J. J., Landmann, J., Machguth, H., Maussion, F., and Pandit, A.: A consensus estimate for the ice thickness distribution of all glaciers on Earth, Nature Geoscience, 12, 168–173, https://doi.org/10.1038/s41561-019-0300-3, 2019a.

Farinotti, D., Round, V., Huss, M., Compagno, L., and Zekollari, H.: Large hydropower and water-storage potential in future glacier-free basins, Nature, 575, 341–344, https://doi.org/10.1038/s41586-019-1740-z, 2019b.

Farinotti, D., Brinkerhoff, D. J., Fürst, J. J., Gantayat, P., Gillet-Chaulet, F., Huss, M., Leclercq, P. W., Maurer, H., Morlighem, M., Pandit, A., Rabatel, A., Ramsankaran, R., Reerink, T. J., Robo, E., Rouges, E., Tamre, E., van Pelt, W. J. J., Werder, M. A., Azam, M. F., Li, H., and Andreassen, L. M.: Results from the Ice Thickness Models Intercomparison eXperiment Phase 2 (ITMIX2), Frontiers in Earth Science, 8, https://doi.org/10.3389/feart.2020.571923, 2021.

Farr, T. G. and Kobrick, M.: Shuttle radar topography mission produces a wealth of data, Eos, Transactions American Geophysical Union, 81, 583–585, https://doi.org/10.1029/EO081i048p00583, 2000.
Felikson, D., Rounce, D., Fasullo, J., Adhikari, S., Dangendorf, S., Kopp, R. E., Reager, J. T., Brinkerhoff, D., Csatho, B., Girotto, M., Hamlington, B., Ivins, E., Larour, E., Nerem, S., Nowicki, S., Schlegel, N. J., Tesdal, J.-E., Rodriguez, A., Buzzanga, B., Lammers, R. B., Kumar, P., and Weathers, M.: Progress and outlook for constraining uncertainties in sea-level projections using observations, https://doi.org/10.22541/essoar.174940490.07639698/v1, 2025.
Flowers, G. E. and Clarke, G. K. C.: Surface and bed topography of Trapridge Glacier, Yukon Territory, Canada: digital elevation models and derived hydraulic geometry, Journal of Glaciology, 45, 165–174, https://doi.org/10.3189/S0022143000003142, 1999.
Freeman, A., Pi, X., and Heggy, E.: Radar Sounding Through the Earth's Ionosphere at 45 MHz, IEEE Transactions on Geoscience and Remote Sensing, 55, 5833–5842, https://doi.org/10.1109/TGRS.2017.2715838, 2017.
Frey, H. and Paul, F.: On the suitability of the SRTM DEM and ASTER GDEM for the compilation of topographic parameters in glacier inventories, International Journal of Applied Earth Observation and Geoinformation, 18, 480–490, https://doi.org/10.1016/j.jag.2011.09.020, 2012.
Frey, H., Machguth, H., Huss, M., Huggel, C., Bajracharya, S., Bolch, T., Kulkarni, A., Linsbauer, A., Salzmann, N., and Stoffel, M.: Estimating the volume of glaciers in the Himalayan-Karakoram region using different methods, The Cryosphere, 8, 2313–2333, https://doi.org/10.5194/tc-8-2313-2014, 2014.
Fürst, J. J., Gillet-Chaulet, F., Benham, T. J., Dowdeswell, J. A., Grabiec, M., Navarro, F., Pettersson, R., Moholdt, G., Nuth, C., Sass, B., Aas, K., Fettweis, X., Lang, C., Seehaus, T., and Braun, M.: Application of a two-step approach for mapping ice thickness to various glacier types on Svalbard, The Cryosphere, 11, 2003–2032, https://doi.org/10.5194/tc-11-2003-2017, 2017.
Fürst, J. J., Navarro, F., Gillet-Chaulet, F., Huss, M., Moholdt, G., Fettweis, X., Lang, C., Seehaus, T., Ai, S., Benham, T. J., Benn, D. I., Björnsson, H., Dowdeswell, J. A., Grabiec, M., Kohler, J., Lavrentiev, I., Lindbäck, K., Melvold, K., Pettersson, R., Rippin, D., Saintenoy, A., Sánchez-Gámez, P., Schuler, T. V., Sevestre, H., Vasilenko, E., and Braun, M. H.: The Ice-Free Topography of Svalbard, Geophysical Research Letters, 45, 11,760–11,769, https://doi.org/10.1029/2018GL079734, 2018.
Fürst, J. J., Farías-Barahona, D., Blindow, N., Casassa, G., Gacitúa, G., Koppes, M., Lodolo, E., Millan, R., Minowa, M., Mouginot, J., Petlicki, M., Rignot, E., Rivera, A., Skvarca, P., Stuefer, M., Sugiyama, S., Uribe, J., Zamora, R., Braun, M. H., Gillet-Chaulet, F., Malz, P., Meier, W. J.-H., and Schaefer, M.: The foundations of the Patagonian icefields, Communications Earth & Environment, 5, 1–10, https://doi.org/10.1038/s43247-023-01193-7, 2024.
Gantayat, P., Kulkarni, A. V., and Srinivasan, J.: Estimation of ice thickness using surface velocities and slope: case study at Gangotri Glacier, India, Journal of Glaciology, 60, 277–282, https://doi.org/10.3189/2014JoG13J078, 2014.
Gardner, A., Fahnestock, M., and Scambos, T.: MEaSUREs ITS_LIVE Landsat Image-Pair Glacier and Ice Sheet Surface Velocities, Version 1,

https://doi.org/10.5067/IMR9D3PEI28U, 2022.
GlaThiDa Consortium: Glacier Thickness Database 3.1.0, URL DOI:10.5904/wgms-glathida-2020-10, 2020.
Glen, J. W.: The creep of polycrystalline ice, Proceedings of the Royal Society of London. Series A. Mathematical and Physical Sciences, 228, 519–538, 1955.
Goldberg, D. N. and Heimbach, P.: Parameter and state estimation with a time-dependent adjoint marine ice sheet model, The Cryosphere, 7, 1659–1678, https://doi.org/10.5194/tc-7-1659-2013, 2013.
Goodfellow, I., Bengio, Y., and Courville, A.: Deep Learning, MIT Press, 2016.
Grab, M., Mattea, E., Bauder, A., Huss, M., Rabenstein, L., Hodel, E., Linsbauer, A., Langhammer, L., Schmid, L., Church, G., Hellmann, S., Délèze, K., Schaer, P., Lathion, P., Farinotti, D., and Maurer, H.: Ice thickness distribution of all Swiss glaciers based on extended ground-penetrating radar data and glaciological modeling, Journal of Glaciology, 67, 1074–1092, https://doi.org/10.1017/jog.2021.55, 2021.
Greve, R. and Blatter, H.: Dynamics of ice sheets and glaciers, Advances in geophysical and environmental mechanics and mathematics, Springer, Dordrecht; New York, 2009.
Grinsted, A.: An estimate of global glacier volume, The Cryosphere, 7, 141–151, https://doi.org/10.5194/tc-7-141-2013, 2013.
Gudmundsson, G. H.: Transmission of basal variability to a glacier surface, Journal of Geophysical Research: Solid Earth, 108, https://doi.org/10.1029/2002JB002107, 2003.
Gudmundsson, G. H. and Raymond, M.: On the limit to resolution and information on basal properties obtainable from surface data on ice streams, The Cryosphere, 2, 167–178, https://doi.org/10.5194/tc-2-167-2008, 2008.
Gärtner-Roer, I., Naegeli, K., Huss, M., Knecht, T., Machguth, H., and Zemp, M.: A database of worldwide glacier thickness observations, Global and Planetary Change, 122, 330–344, https://doi.org/10.1016/j.gloplacha.2014.09.003, 2014.
Habermann, M., Maxwell, D., and Truffer, M.: Reconstruction of basal properties in ice sheets using iterative inverse methods, Journal of Glaciology, 58, 795–808, https://doi.org/10.3189/2012JoG11J168, 2012.
He, Q., Perego, M., Howard, A. A., Karniadakis, G. E., and Stinis, P.: A hybrid deep neural operator/finite element method for ice-sheet modeling, Journal of Computational Physics, 492, 112 428, https://doi.org/10.1016/j.jcp.2023.112428, 2023.
Heining, C.: Velocity field reconstruction in gravity-driven flow over unknown topography, Physics of Fluids, 23, 032 101, https://doi.org/10.1063/1.3559144, 2011.
Herrmann, O., Groos, A. R., Tabone, I., Jouvet, G., and Fürst, J. J.: A Kalman filter-based framework for assimilating remote sensing observations into a surface mass balance model, Annals of Glaciology, 66, e23, https://doi.org/10.1017/aog.2025.10020, 2025.
Hindmarsh, R. C.: Qualitative dynamics of marine ice sheets, in: Ice in the climate system, pp. 67–99, Springer, 1993.
Hindmarsh, R. C.: The stability of a viscous till sheet coupled with ice flow, considered at wavelengths less than the ice thickness, Journal of Glaciology, 44,

285–292, 1998.
Hock, R., Bliss, A., Marzeion, B., Giesen, R. H., Hirabayashi, Y., Huss, M., Radić, V., and Slangen, A. B. A.: GlacierMIP – A model intercomparison of global-scale glacier mass-balance models and projections, Journal of Glaciology, 65, 453–467, https://doi.org/10.1017/jog.2019.22, 2019.
Hock, R., Maussion, F., Marzeion, B., and Nowicki, S.: What is the global glacier ice volume outside the ice sheets?, Journal of Glaciology, 69, 204–210, https://doi.org/10.1017/jog.2023.1, 2023.
Hodson, A., Anesio, A. M., Tranter, M., Fountain, A., Osborn, M., Priscu, J., Laybourn-Parry, J., and Sattler, B.: Glacial Ecosystems, Ecological Monographs, 78, 41–67, https://doi.org/10.1890/07-0187.1, 2008.
Hodson, A. J. and Ferguson, R. I.: Fluvial suspended sediment transport from cold and warm-based glaciers in Svalbard, Earth Surface Processes and Landforms, 24, 957–974, 1999.
Hooke, R. L.: Principles of glacier mechanics, Cambridge University Press, New York, 2005.
Hugonnet, R., McNabb, R., Berthier, E., Menounos, B., Nuth, C., Girod, L., Farinotti, D., Huss, M., Dussaillant, I., Brun, F., and Kääb, A.: Accelerated global glacier mass loss in the early twenty-first century, Nature, 592, 726–731, https://doi.org/10.1038/s41586-021-03436-z, 2021.
Huss, M.: Density assumptions for converting geodetic glacier volume change to mass change, The Cryosphere, 7, 877–887, 2013.
Huss, M. and Farinotti, D.: Distributed ice thickness and volume of all glaciers around the globe, Journal of Geophysical Research: Earth Surface, 117, https://doi.org/10.1029/2012JF002523, 2012.
Huss, M. and Hock, R.: A new model for global glacier change and sea-level rise, Frontiers in Earth Science, 3, https://doi.org/10.3389/feart.2015.00054, 2015.
Huss, M. and Hock, R.: Global-scale hydrological response to future glacier mass loss, Nature Climate Change, 8, 135–140, https://doi.org/10.1038/s41558-017-0049-x, 2018.
Huss, M., Jouvet, G., Farinotti, D., and Bauder, A.: Future high-mountain hydrology: a new parameterization of glacier retreat, Hydrology and Earth System Sciences, 14, 815–829, https://doi.org/10.5194/hess-14-815-2010, 2010.
Hutter, K.: The Effect of Longitudinal Strain on the Shear Stress of an Ice Sheet: In Defence of Using Stretched Coordinates, Journal of Glaciology, 27, 39–56, https://doi.org/10.3189/S0022143000011217, 1981.
Hutter, K.: Theoretical glaciology: materials science of ice and the mechanics of glaciers and ice sheets, Mathematical approaches to geophysics, Reidel, Dordrecht, 1983.
Immerzeel, W. W., Lutz, A. F., Andrade, M., Bahl, A., Biemans, H., Bolch, T., Hyde, S., Brumby, S., Davies, B. J., Elmore, A. C., Emmer, A., Feng, M., Fernández, A., Haritashya, U., Kargel, J. S., Koppes, M., Kraaijenbrink, P. D. A., Kulkarni, A. V., Mayewski, P. A., Nepal, S., Pacheco, P., Painter, T. H., Pellicciotti, F., Rajaram, H., Rupper, S., Sinisalo, A., Shrestha, A. B., Viviroli, D., Wada, Y., Xiao, C., Yao, T., and Baillie, J. E. M.: Importance and vulnerability of the world's water towers, Nature, 577, 364–369, https://doi.org/10.1038/s41586-019-1822-y, 2020.

IPCC: Climate Change 2021: The Physical Science Basis. Contribution of Working Group I to the Sixth Assessment Report of the Intergovernmental Panel on Climate Change, Cambridge University Press, Cambridge, United Kingdom and New York, NY, USA, https://doi.org/10.1017/9781009157896, 2021.

Jouvet, G.: Inversion of a Stokes glacier flow model emulated by deep learning, Journal of Glaciology, 69, 13–26, https://doi.org/10.1017/jog.2022.41, 2023.

Jouvet, G. and Cordonnier, G.: Ice-flow model emulator based on physics-informed deep learning, Journal of Glaciology, pp. 1–15, https://doi.org/10.1017/jog.2023.73, 2023.

Jouvet, G., Picasso, M., Rappaz, J., and Blatter, H.: A new algorithm to simulate the dynamics of a glacier: theory and applications, Journal of Glaciology, 54, 801–811, https://doi.org/10.3189/002214308787780049, 2008.

Jouvet, G., Cordonnier, G., Kim, B., Lüthi, M., Vieli, A., and Aschwanden, A.: Deep learning speeds up ice flow modelling by several orders of magnitude, Journal of Glaciology, 68, 651–664, https://doi.org/10.1017/jog.2021.120, 2022.

Kamb, B. and Echelmeyer, K. A.: Stress-Gradient Coupling in Glacier Flow: I. Longitudinal Averaging of the Influence of Ice Thickness and Surface Slope, Journal of Glaciology, 32, 267–284, https://doi.org/10.3189/S0022143000015604, 1986.

Karlsson, N. B., Solgaard, A. M., Mankoff, K. D., Gillet-Chaulet, F., MacGregor, J. A., Box, J. E., Citterio, M., Colgan, W. T., Larsen, S. H., Kjeldsen, K. K., Korsgaard, N. J., Benn, D. I., Hewitt, I. J., and Fausto, R. S.: A first constraint on basal melt-water production of the Greenland ice sheet, Nature Communications, 12, 3461, https://doi.org/10.1038/s41467-021-23739-z, 2021.

Kartverket: Height DTM 50 m, URL `https://kartkatalog.geonorge.no/metadata/height-dtm-50/e25d0104-0858-4d06-bba8-d154514c11d2#help-info`, 2013.

Kavan, J., Luláková, P., Małecki, J., and Strzelecki, M. C.: Capturing the transition from marine to land-terminating glacier from the 126-year retreat history of Nordenskiöldbreen, Svalbard, Journal of Glaciology, pp. 1–11, https://doi.org/10.1017/jog.2023.92, 2023.

Kirchner, N., Ahlkrona, J., Gowan, E. J., Lötstedt, P., Lea, J. M., Noormets, R., von Sydow, L., Dowdeswell, J. A., and Benham, T.: Shallow ice approximation, second order shallow ice approximation, and full Stokes models: A discussion of their roles in palaeo-ice sheet modelling and development, Quaternary Science Reviews, 147, 136–147, https://doi.org/10.1016/j.quascirev.2016.01.032, 2016.

Kitanidis, P. K.: Introduction to Geostatistics: Applications in Hydrogeology, Cambridge University Press, 1997.

Kneib, M., Dehecq, A., Gilbert, A., Basset, A., Miles, E. S., Jouvet, G., Jourdain, B., Ducasse, E., Beraud, L., Rabatel, A., Mouginot, J., Carcanade, G., Laarman, O., Brun, F., and Six, D.: Distributed surface mass balance of an avalanche-fed glacier, The Cryosphere, 18, 5965–5983, https://doi.org/10.5194/tc-18-5965-2024, 2024.

Koch, M., Seehaus, T., Friedl, P., and Braun, M.: Automated Detection of Glacier Surges from Sentinel-1 Surface Velocity Time Series—An Example from Svalbard, Remote Sensing, 15, 1545, https://doi.org/10.3390/rs15061545, 2023.

Kochtitzky, W., Copland, L., Van Wychen, W., Hugonnet, R., Hock, R., Dowdeswell, J. A., Benham, T., Strozzi, T., Glazovsky, A., Lavrentiev, I., Rounce, D. R., Millan,

R., Cook, A., Dalton, A., Jiskoot, H., Cooley, J., Jania, J., and Navarro, F.: The unquantified mass loss of Northern Hemisphere marine-terminating glaciers from 2000–2020, Nature Communications, 13, 5835, https://doi.org/10.1038/s41467-022-33231-x, 2022.

Koo, Y. and Rahnemoonfar, M.: Graph convolutional network as a fast statistical emulator for numerical ice sheet modeling, Journal of Glaciology, 71, e15, https://doi.org/10.1017/jog.2024.93, 2025.

Lantmäteriet: Markhöjdmodell Nedladdning, grid 50+, URL https://www.lantmateriet.se/sv/geodata/vara-produkter/produktlista/markhojdmodell-nedladdning-grid-50/#anchor-1, 2022.

LeCun, Y., Bengio, Y., and Hinton, G.: Deep learning, Nature, 521, 436–444, https://doi.org/10.1038/nature14539, 2015.

Leger, T. P. M., Jouvet, G., Kamleitner, S., Mey, J., Herman, F., Finley, B. D., Ivy-Ochs, S., Vieli, A., Henz, A., and Nussbaumer, S. U.: A data-consistent model of the last glaciation in the Alps achieved with physics-driven AI, Nature Communications, 16, 848, https://doi.org/10.1038/s41467-025-56168-3, 2025.

Linsbauer, A., Paul, F., and Haeberli, W.: Modeling glacier thickness distribution and bed topography over entire mountain ranges with GlabTop: Application of a fast and robust approach, Journal of Geophysical Research: Earth Surface, 117, https://doi.org/10.1029/2011JF002313, 2012.

Linsbauer, A., Frey, H., Haeberli, W., Machguth, H., Azam, M. F., and Allen, S.: Modelling glacier-bed overdeepenings and possible future lakes for the glaciers in the Himalaya—Karakoram region, Annals of Glaciology, 57, 119–130, https://doi.org/10.3189/2016AoG71A627, 2016.

Liu, J., Wu, Y., and Gao, X.: Increase in occurrence of large glacier-related landslides in the high mountains of Asia, Scientific Reports, 11, 1635, https://doi.org/10.1038/s41598-021-81212-9, 2021.

MacAyeal, D. R.: Large-scale ice flow over a viscous basal sediment: Theory and application to ice stream B, Antarctica, Journal of Geophysical Research: Solid Earth, 94, 4071–4087, https://doi.org/10.1029/JB094iB04p04071, 1989.

MacAyeal, D. R.: The basal stress distribution of Ice Stream E, Antarctica, inferred by control methods, Journal of Geophysical Research: Solid Earth, 97, 595–603, https://doi.org/10.1029/91JB02454, 1992.

MacAyeal, D. R.: A tutorial on the use of control methods in ice-sheet modeling, Journal of Glaciology, 39, 91–98, https://doi.org/10.3189/S0022143000015744, 1993.

Magnússon, E., Björnsson, H., Dall, J., and Pálsson, F.: Volume changes of Vatnajökull ice cap, Iceland, due to surface mass balance, ice flow, and subglacial melting at geothermal areas, Geophysical Research Letters, 32, https://doi.org/10.1029/2004GL021615, 2005.

Marzeion, B., Jarosch, A. H., and Hofer, M.: Past and future sea-level change from the surface mass balance of glaciers, The Cryosphere, 6, 1295–1322, https://doi.org/10.5194/tc-6-1295-2012, 2012.

Maussion, F., Butenko, A., Champollion, N., Dusch, M., Eis, J., Fourteau, K., Gregor, P., Jarosch, A. H., Landmann, J., Oesterle, F., Recinos, B., Rothenpieler, T., Vlug, A., Wild, C. T., and Marzeion, B.: The Open Global Glacier Model (OGGM) v1.1, Geoscientific Model Development, 12, 909–931,

https://doi.org/10.5194/gmd-12-909-2019, 2019.
Meehl, G. A., Boer, G. J., Covey, C., Latif, M., and Stouffer, R. J.: The Coupled Model Intercomparison Project (CMIP), Bulletin of the American Meteorological Society, 81, 313–318, URL https://www.jstor.org/stable/26215108, 2000.
Michel, L., Picasso, M., Farinotti, D., Bauder, A., Funk, M., and Blatter, H.: Estimating the ice thickness of mountain glaciers with an inverse approach using surface topography and mass-balance, Inverse Problems, 29, 035 002, https://doi.org/10.1088/0266-5611/29/3/035002, 2013.
Millan, R., Mouginot, J., Rabatel, A., and Morlighem, M.: Ice velocity and thickness of the world's glaciers, Nature Geoscience, 15, 124–129, https://doi.org/10.1038/s41561-021-00885-z, 2022.
Morin, A., Flowers, G. E., Nolan, A., Brinkerhoff, D., and Berthier, E.: Exploiting high-slip flow regimes to improve inference of glacier bed topography, Journal of Glaciology, 69, 658–664, https://doi.org/10.1017/jog.2022.121, 2023.
Morland, L. W.: Unconfined ice-shelf flow, in: Van der Veen C.J., Oerlemans J. (eds) Dynamics of the West Antarctic Ice Sheet, vol. 4 of *Glaciology and Quaternary Geology*, pp. 99–116, Springer, Dodrecht, 1987.
Morlighem, M., Rignot, E., Seroussi, H., Larour, E., Dhia, H. B., and Aubry, D.: A mass conservation approach for mapping glacier ice thickness, Geophysical Research Letters, 38, https://doi.org/https://doi.org/10.1029/2011GL048659, 2011.
Morlighem, M., Williams, C. N., Rignot, E., An, L., Arndt, J. E., Bamber, J. L., Catania, G., Chauché, N., Dowdeswell, J. A., Dorschel, B., Fenty, I., Hogan, K., Howat, I., Hubbard, A., Jakobsson, M., Jordan, T. M., Kjeldsen, K. K., Millan, R., Mayer, L., Mouginot, J., Noël, B. P. Y., O'Cofaigh, C., Palmer, S., Rysgaard, S., Seroussi, H., Siegert, M. J., Slabon, P., Straneo, F., van den Broeke, M. R., Weinrebe, W., Wood, M., and Zinglersen, K. B.: BedMachine v3: Complete Bed Topography and Ocean Bathymetry Mapping of Greenland From Multibeam Echo Sounding Combined With Mass Conservation, Geophysical Research Letters, 44, 11,051–11,061, https://doi.org/10.1002/2017GL074954, 2017.
Morlighem, M., Rignot, E., Binder, T., Blankenship, D., Drews, R., Eagles, G., Eisen, O., Ferraccioli, F., Forsberg, R., Fretwell, P., Goel, V., Greenbaum, J. S., Gudmundsson, H., Guo, J., Helm, V., Hofstede, C., Howat, I., Humbert, A., Jokat, W., Karlsson, N. B., Lee, W. S., Matsuoka, K., Millan, R., Mouginot, J., Paden, J., Pattyn, F., Roberts, J., Rosier, S., Ruppel, A., Seroussi, H., Smith, E. C., Steinhage, D., Sun, B., Broeke, M. R. v. d., Ommen, T. D. v., Wessem, M. v., and Young, D. A.: Deep glacial troughs and stabilizing ridges unveiled beneath the margins of the Antarctic ice sheet, Nature Geoscience, 13, 132–137, https://doi.org/10.1038/s41561-019-0510-8, 2020.
Neven, A., Dall'Alba, V., Juda, P., Straubhaar, J., and Renard, P.: Ice volume and basal topography estimation using geostatistical methods and ground-penetrating radar measurements: application to the Tsanfleuron and Scex Rouge glaciers, Swiss Alps, The Cryosphere, 15, 5169–5186, https://doi.org/10.5194/tc-15-5169-2021, 2021.
Nogueira, F.: Bayesian Optimization: Open source constrained global optimization tool for Python, URL https://github.com/bayesian-optimization/BayesianOptimization, 2014.

Noël, B., Jakobs, C. L., van Pelt, W. J. J., Lhermitte, S., Wouters, B., Kohler, J., Hagen, J. O., Luks, B., Reijmer, C. H., van de Berg, W. J., and van den Broeke, M. R.: Low elevation of Svalbard glaciers drives high mass loss variability, Nature Communications, 11, 4597, https://doi.org/10.1038/s41467-020-18356-1, 2020.
NPI: Terrengmodell Svalbard (S0 Terrengmodell), https://doi.org/10.21334/NPOLAR.2014.DCE53A47, 2014.
Nuth, C., Kohler, J., König, M., Deschwanden, A. v., Hagen, J. O., Kääb, A., Moholdt, G., and Pettersson, R.: Decadal changes from a multi-temporal glacier inventory of Svalbard, The Cryosphere, 7, 1603–1621, https://doi.org/https://doi.org/10.5194/tc-7-1603-2013, 2013.
Nye, J. F.: The flow of glaciers and ice-sheets as a problem in plasticity, Proceedings of the Royal Society of London. Series A. Mathematical and Physical Sciences, 207, 554–572, 1951.
Nye, J. F.: A Method of Calculating the Thicknesses of the Ice-Sheets, Nature, 169, 529–530, https://doi.org/10.1038/169529a0, 1952.
Oerlemans, J.: The microclimate of valley glaciers, Igitur, Utrecht Publishing & Archiving Services, URL https://dspace.library.uu.nl/handle/1874/42854, 2010.
Ohmura, A.: Cryosphere during the twentieth century, The state of the planet: frontiers and challenges in geophysics, 150, 239–257, URL https://www.researchgate.net/profile/Atsumu-Ohmura-2/publication/245820334_Cryosphere_During_the_Twentieth_Century/links/579a1abf08ae2e0b31b14878/Cryosphere-During-the-Twentieth-Century.pdf, 2004.
Pattyn, F.: A new three-dimensional higher-order thermomechanical ice sheet model: Basic sensitivity, ice stream development, and ice flow across subglacial lakes, Journal of Geophysical Research: Solid Earth, 108, https://doi.org/10.1029/2002JB002329, 2003.
Pfeffer, W. T., Arendt, A. A., Bliss, A., Bolch, T., Cogley, J. G., Gardner, A. S., Hagen, J.-O., Hock, R., Kaser, G., Kienholz, C., Miles, E. S., Moholdt, G., Mölg, N., Paul, F., Radić, V., Rastner, P., Raup, B. H., Rich, J., Sharp, M. J., and Consortium, T. R.: The Randolph Glacier Inventory: a globally complete inventory of glaciers, Journal of Glaciology, 60, 537–552, https://doi.org/10.3189/2014JoG13J176, 2014.
Pohjola, V. A.: TV-video observations of bed and basal sliding on Storglaciären, Sweden, Journal of Glaciology, 39, 111–118, https://doi.org/10.3189/S0022143000015768, 1993.
Pritchard, H. D.: Asia's shrinking glaciers protect large populations from drought stress, Nature, 569, 649–654, 2019.
Radić, V. and Hock, R.: Regional and global volumes of glaciers derived from statistical upscaling of glacier inventory data, Journal of Geophysical Research: Earth Surface, 115, https://doi.org/https://doi.org/10.1029/2009JF001373, 2010.
Radić, V. and Hock, R.: Regionally differentiated contribution of mountain glaciers and ice caps to future sea-level rise, Nature Geoscience, 4, 91–94, https://doi.org/10.1038/ngeo1052, 2011.
Radić, V. and Hock, R.: Glaciers in the Earth's Hydrological Cycle: Assessments of Glacier Mass and Runoff Changes on Global and Regional Scales, Surveys in

Geophysics, 35, 813–837, https://doi.org/10.1007/s10712-013-9262-y, 2014.
Radić, V., Bliss, A., Beedlow, A. C., Hock, R., Miles, E., and Cogley, J. G.: Regional and global projections of twenty-first century glacier mass changes in response to climate scenarios from global climate models, Climate Dynamics, 42, 37–58, https://doi.org/10.1007/s00382-013-1719-7, 2014.
Raper, S. C. B. and Braithwaite, R. J.: The potential for sea level rise: New estimates from glacier and ice cap area and volume distributions, Geophysical Research Letters, 32, https://doi.org/10.1029/2004GL021981, 2005.
Raymond, M. J. and Gudmundsson, G. H.: On the relationship between surface and basal properties on glaciers, ice sheets, and ice streams, Journal of Geophysical Research: Solid Earth, 110, https://doi.org/10.1029/2005JB003681, 2005.
Recinos, B., Maussion, F., Noël, B., Möller, M., and Marzeion, B.: Calibration of a frontal ablation parameterisation applied to Greenland's peripheral calving glaciers, Journal of Glaciology, 67, 1177–1189, https://doi.org/10.1017/jog.2021.63, 2021.
RGI Consortium: Randolph Glacier Inventory – A Dataset of Global Glacier Outlines: Version 6.0, NSIDC: National Snow and Ice Data Center, Boulder, Colorado USA, URL https://doi.org/10.7265/N5-RGI-60, 2017.
Rounce, D. R., Hock, R., McNabb, R. W., Millan, R., Sommer, C., Braun, M. H., Malz, P., Maussion, F., Mouginot, J., Seehaus, T. C., and Shean, D. E.: Distributed Global Debris Thickness Estimates Reveal Debris Significantly Impacts Glacier Mass Balance, Geophysical Research Letters, 48, e2020GL091 311, https://doi.org/10.1029/2020GL091311, 2021.
Rounce, D. R., Hock, R., Maussion, F., Hugonnet, R., Kochtitzky, W., Huss, M., Berthier, E., Brinkerhoff, D., Compagno, L., Copland, L., Farinotti, D., Menounos, B., and McNabb, R. W.: Global glacier change in the 21st century: Every increase in temperature matters, Science, 379, 78–83, https://doi.org/10.1126/science.abo1324, 2023.
Sattar, A., Cook, K. L., Rai, S. K., Berthier, E., Allen, S., Rinzin, S., de Vries, M. V. W., Haeberli, W., Kushwaha, P., Shugar, D. H., Emmer, A., Haritashya, U. K., Frey, H., Rao, P., Gurudin, K. S. K., Rai, P., Rajak, R., Hossain, F., Huggel, C., Mergili, M., Azam, M. F., Gascoin, S., Carrivick, J. L., Bell, L. E., Ranjan, R. K., Rashid, I., Kulkarni, A. V., Petley, D., Schwanghart, W., Watson, C. S., Islam, N., Gupta, M. D., Lane, S. N., and Bhat, S. Y.: The Sikkim flood of October 2023: Drivers, causes, and impacts of a multihazard cascade, Science, 387, eads2659, https://doi.org/10.1126/science.ads2659, 2025.
Schaefer, J. M., Finkel, R. C., Balco, G., Alley, R. B., Caffee, M. W., Briner, J. P., Young, N. E., Gow, A. J., and Schwartz, R.: Greenland was nearly ice-free for extended periods during the Pleistocene, Nature, 540, 252–255, https://doi.org/10.1038/nature20146, 2016.
Schmitt, P., Maussion, F., Goldberg, D. N., and Gregor, P.: The Open Global Glacier Data Assimilation Framework (AGILE) v0.1, EGUsphere, pp. 1–35, https://doi.org/10.5194/egusphere-2025-3401, 2025.
Schoof, C.: Ice-sheet acceleration driven by melt supply variability, Nature, 468, 803–806, https://doi.org/10.1038/nature09618, 2010.
Schuler, T. V., Benestad, R. E., Isaksen, K., Kierulf, H. P., Kohler, J., Moholdt, G., and Schmidt, L. S.: Svalbard's 2024 record summer: An early view of Arctic

glacier meltdown?, Proceedings of the National Academy of Sciences, 122, e2503806 122, https://doi.org/10.1073/pnas.2503806122, 2025.
Schuster, L., Rounce, D. R., and Maussion, F.: Glacier projections sensitivity to temperature-index model choices and calibration strategies, Annals of Glaciology, 64, 293–308, https://doi.org/10.1017/aog.2023.57, 2023.
Schuster, L., Maussion, F., Rounce, D. R., Ultee, L., Schmitt, P., Lacroix, F., Frölicher, T. L., and Schleussner, C.-F.: Irreversible glacier change and trough water for centuries after overshooting 1.5 °C, Nature Climate Change, 15, 634–641, https://doi.org/10.1038/s41558-025-02318-w, 2025.
Seroussi, H., Nowicki, S., Payne, A. J., Goelzer, H., Lipscomb, W. H., Abe-Ouchi, A., Agosta, C., Albrecht, T., Asay-Davis, X., Barthel, A., Calov, R., Cullather, R., Dumas, C., Galton-Fenzi, B. K., Gladstone, R., Golledge, N. R., Gregory, J. M., Greve, R., Hattermann, T., Hoffman, M. J., Humbert, A., Huybrechts, P., Jourdain, N. C., Kleiner, T., Larour, E., Leguy, G. R., Lowry, D. P., Little, C. M., Morlighem, M., Pattyn, F., Pelle, T., Price, S. F., Quiquet, A., Reese, R., Schlegel, N.-J., Shepherd, A., Simon, E., Smith, R. S., Straneo, F., Sun, S., Trusel, L. D., Van Breedam, J., van de Wal, R. S. W., Winkelmann, R., Zhao, C., Zhang, T., and Zwinger, T.: ISMIP6 Antarctica: a multi-model ensemble of the Antarctic ice sheet evolution over the 21st century, The Cryosphere, 14, 3033–3070, https://doi.org/10.5194/tc-14-3033-2020, 2020.
Serreze, M. C. and Barry, R. G.: Processes and impacts of Arctic amplification: A research synthesis, Global and Planetary Change, 77, 85–96, https://doi.org/10.1016/j.gloplacha.2011.03.004, 2011.
Shahateet, K., J. Fürst, J., Navarro, F., Seehaus, T., Farinotti, D., and Braun, M.: A reconstruction of the ice thickness of the Antarctic Peninsula Ice Sheet north of 70° S, The Cryosphere, 19, 1577–1597, https://doi.org/10.5194/tc-19-1577-2025, 2025.
Skidmore, M. L., Foght, J. M., and Sharp, M. J.: Microbial Life beneath a High Arctic Glacier, Applied and Environmental Microbiology, 66, 3214–3220, https://doi.org/10.1128/AEM.66.8.3214-3220.2000, 2000.
Stroeven, A. P., Hättestrand, C., Kleman, J., Heyman, J., Fabel, D., Fredin, O., Goodfellow, B. W., Harbor, J. M., Jansen, J. D., and Olsen, L.: Deglaciation of Fennoscandia, Quaternary Science Reviews, 147, 91–121, 2016.
Susstrunk, A.: Sondage du Glacier par la Méthode Sismique, La Houille Blanche, 37, 309–318, https://doi.org/10.1051/lhb/1951010, 1951.
Terleth, Y., Pelt, W. J. J. v., and Pettersson, R.: Spatial variability in winter mass balance on Storglaciären modelled with a terrain-based approach, Journal of Glaciology, 69, 749–761, https://doi.org/10.1017/jog.2022.96, 2023.
Utkin, I., Chen, Y., Räss, L., and Werder, M. A.: Snapshot and time-dependent inversions of basal sliding using automatic generation of adjoint code on graphics processing units, Journal of Glaciology, 71, e72, https://doi.org/10.1017/jog.2025.40, 2025.
Vallot, D., Pettersson, R., Luckman, A., Benn, D. I., Zwinger, T., Pelt, W. J. J. V., Kohler, J., Schäfer, M., Claremar, B., and Hulton, N. R. J.: Basal dynamics of Kronebreen, a fast-flowing tidewater glacier in Svalbard: non-local spatio-temporal response to water input, Journal of Glaciology, 63, 1012–1024, https://doi.org/10.1017/jog.2017.69, 2017.

van Pelt, W. J. J., Oerlemans, J., Reijmer, C. H., Pettersson, R., Pohjola, V. A., Isaksson, E., and Divine, D.: An iterative inverse method to estimate basal topography and initialize ice flow models, The Cryosphere, 7, 987–1006, https://doi.org/10.5194/tc-7-987-2013, 2013.
van Pelt, W. J. J., Pohjola, V., Pettersson, R., Marchenko, S., Kohler, J., Luks, B., Hagen, J. O., Schuler, T. V., Dunse, T., Noël, B., and Reijmer, C.: A long-term dataset of climatic mass balance, snow conditions, and runoff in Svalbard (1957–2018), The Cryosphere, 13, 2259–2280, https://doi.org/10.5194/tc-13-2259-2019, 2019.
van Pelt, W. J. J., Schuler, T. V., Pohjola, V. A., and Pettersson, R.: Accelerating future mass loss of Svalbard glaciers from a multi-model ensemble, Journal of Glaciology, 67, 485–499, https://doi.org/10.1017/jog.2021.2, 2021.
Vanlooy, J. A., Miège, C., Vandeberg, G. S., and Forster, R. R.: Ice volume estimation inferred from ice thickness and surface measurements for Continental Glacier, Wind River Range, Wyoming, USA, Journal of Glaciology, 60, 478–488, https://doi.org/10.3189/2014JoG13J162, 2014.
Walker, S.: Everything We Know About GPT-4 — Klu, URL `https://klu.ai/blog/gpt-4-llm`, 2024.
Wang, Y., Lai, C.-Y., Prior, D. J., and Cowen-Breen, C.: Deep learning the flow law of Antarctic ice shelves, Science, 387, 1219–1224, https://doi.org/10.1126/science.adp3300, 2025.
Weertman, J.: On the sliding of glaciers, Journal of glaciology, 3, 33–38, 1957.
Welty, E., Zemp, M., Navarro, F., Huss, M., Fürst, J. J., Gärtner-Roer, I., Landmann, J., Machguth, H., Naegeli, K., Andreassen, L. M., Farinotti, D., Li, H., and GlaThiDa Contributors: Worldwide version-controlled database of glacier thickness observations, Earth System Science Data, 12, 3039–3055, https://doi.org/10.5194/essd-12-3039-2020, 2020.
WGMS: Fluctuations of Glaciers Database, https://doi.org/10.5904/wgms-fog-2022-09, 2022.
Xu, J., Grumbine, R. E., Shrestha, A., Eriksson, M., Yang, X., Wang, Y. U. N., and Wilkes, A.: The melting Himalayas: cascading effects of climate change on water, biodiversity, and livelihoods, Conservation Biology, 23, 520–530, 2009.
Zachos, J., Pagani, M., Sloan, L., Thomas, E., and Billups, K.: Trends, rhythms, and aberrations in global climate 65 Ma to present, Science, 292, 686–693, 2001.
Zekollari, H., Huss, M., Farinotti, D., and Lhermitte, S.: Ice-Dynamical Glacier Evolution Modeling—A Review, Reviews of Geophysics, 60, e2021RG000 754, https://doi.org/10.1029/2021RG000754, 2022.
Zekollari, H., Huss, M., Schuster, L., Maussion, F., Rounce, D. R., Aguayo, R., Champollion, N., Compagno, L., Hugonnet, R., Marzeion, B., Mojtabavi, S., and Farinotti, D.: Twenty-first century global glacier evolution under CMIP6 scenarios and the role of glacier-specific observations, The Cryosphere, 18, 5045–5066, https://doi.org/10.5194/tc-18-5045-2024, 2024.
Zekollari, H., Schuster, L., Maussion, F., Hock, R., Marzeion, B., Rounce, D. R., Compagno, L., Fujita, K., Huss, M., James, M., Kraaijenbrink, P. D. A., Lipscomb, W. H., Minallah, S., Oberrauch, M., Van Tricht, L., Champollion, N., Edwards, T., Farinotti, D., Immerzeel, W., Leguy, G., and Sakai, A.: Glacier preservation doubled by limiting warming to 1.5°C versus 2.7°C, Science, 388, 979–983,

https://doi.org/10.1126/science.adu4675, 2025.
Zemp, M., Jakob, L., Dussaillant, I., Nussbaumer, S. U., Gourmelen, N., Dubber, S., A, G., Abdullahi, S., Andreassen, L. M., Berthier, E., Bhattacharya, A., Blazquez, A., Boehm Vock, L. F., Bolch, T., Box, J., Braun, M. H., Brun, F., Cicero, E., Colgan, W., Eckert, N., Farinotti, D., Florentine, C., Floricioiu, D., Gardner, A., Harig, C., Hassan, J., Hugonnet, R., Huss, M., Jóhannesson, T., Liang, C.-C. A., Ke, C.-Q., Khan, S. A., King, O., Kneib, M., Krieger, L., Maussion, F., Mattea, E., McNabb, R., Menounos, B., Miles, E., Moholdt, G., Nilsson, J., Pálsson, F., Pfeffer, J., Piermattei, L., Plummer, S., Richter, A., Sasgen, I., Schuster, L., Seehaus, T., Shen, X., Sommer, C., Sutterley, T., Treichler, D., Velicogna, I., Wouters, B., Zekollari, H., Zheng, W., and The GlaMBIE Team: Community estimate of global glacier mass changes from 2000 to 2023, Nature, 639, 382–388, https://doi.org/10.1038/s41586-024-08545-z, 2025.
Zhang, T., Wang, W., An, B., Gao, T., and Yao, T.: Ice thickness and morphological analysis reveal the future glacial lake distribution and formation probability in the Tibetan Plateau and its surroundings, Global and Planetary Change, 216, 103 923, https://doi.org/10.1016/j.gloplacha.2022.103923, 2022.
Zheng, G., Allen, S. K., Bao, A., Ballesteros-Cánovas, J. A., Huss, M., Zhang, G., Li, J., Yuan, Y., Jiang, L., Yu, T., Chen, W., and Stoffel, M.: Increasing risk of glacial lake outburst floods from future Third Pole deglaciation, Nature Climate Change, 11, 411–417, https://doi.org/10.1038/s41558-021-01028-3, 2021.
Zhou, G., Sun, Z., and Fu, S.: An efficient variant of the Priority-Flood algorithm for filling depressions in raster digital elevation models, Computers & Geosciences, 90, 87–96, https://doi.org/10.1016/j.cageo.2016.02.021, 2016.
Åkesson, H., Nisancioglu, K. H., Giesen, R. H., and Morlighem, M.: Simulating the evolution of Hardangerjøkulen ice cap in southern Norway since the mid-Holocene and its sensitivity to climate change, The Cryosphere, 11, 281–302, https://doi.org/10.5194/tc-11-281-2017, 2017.

Acta Universitatis Upsaliensis

Digital Comprehensive Summaries of Uppsala Dissertations from the Faculty of Science and Technology 2611

Editor: The Dean of the Faculty of Science and Technology

A doctoral dissertation from the Faculty of Science and Technology, Uppsala University, is usually a summary of a number of papers. A few copies of the complete dissertation are kept at major Swedish research libraries, while the summary alone is distributed internationally through the series Digital Comprehensive Summaries of Uppsala Dissertations from the Faculty of Science and Technology. (Prior to January, 2005, the series was published under the title "Comprehensive Summaries of Uppsala Dissertations from the Faculty of Science and Technology".)

Distribution: publications.uu.se
urn:nbn:se:uu:diva-570124

ACTA UNIVERSITATIS
UPSALIENSIS
2026